7-23-2020

Morphology, Taxonomy, and Ecological Niche Modeling of the Cochabamba Grass Mouse, *Akodon siberiae* Myers & Patton, 1989

James George Dunn
Portland State University

Recommended Citation

Morphology, Taxonomy, and Ecological Niche Modeling

of the Cochabamba Grass Mouse,

Akodon siberiae Myers & Patton, 1989

by

James George Dunn

A thesis submitted in partial fulfillment of the
requirements for the degree of

Master of Science
In
Biology

Thesis Committee:
Luis A. Ruedas, Chair
Deborah A. Duffield
Michael T. Murphy
Thomas V. Hancock

Portland State University
2019

Abstract

The Cochabamba Grass Mouse, *Akodon siberiae*, is a small mouse (mean head+body length: 103 mm, $N = 22$) that occurs in a spatially restricted range in the Bolivian Yungas forests, the cloud forest transition zone between lowland Amazonia and the Andean Altiplano. Like many species in the genus, their appearance is very similar to that of other species in the genus: they are difficult to distinguish from their congeners, and are challenging to identify. In the absence of molecular data, *A. siberiae* specimens require a thorough and careful analysis of external and cranial features for identification. Furthermore, *Akodon mimus*, *A. dayi, and A. varius*, resemble *A. siberiae* and overlap its range. In this study, a detailed morphological comparison was carried out of external and cranial features between the sympatric *A. siberiae* and *A. mimus*. A principal component analysis was carried out on cranial measurements of *A. siberiae* and the three sympatric *Akodon* species that it most closely resembles. Two phylogenetic trees were constructed based on molecular data from the mitochondrial cytochrome b gene using 37 of the 39 *Akodon* species to further assess species relationships and the evolutionary relationships of *A. siberiae*. One tree was constructed with all *Akodon* specimens from Genbank and including specimens from this study. Another tree was constructed with one specimen per species for clarity. The morphological comparison revealed a number of key differences between *A. siberiae* and *A. mimus*. From the dentition, I infer that *A. siberiae* has an insect dominated omnivorous diet, in contrast to *A. mimus*, which has a vegetation dominated omnivorous diet. The ecological niche model revealed that even under ideal circumstances, *A. siberiae* only has a small geographical area that it could successfully

inhabit. Habitat loss by anthropogenic development is a major threat to *A. siberiae*. The

evolution and biology of *A. siberiae* appears to be tied to its particular habitat and small

range in the Bolivian Yungas. Continued and enforced protection of those habitats is

necessary to maintain stable populations of *A. siberiae*.

Acknowledgements

Table of Contents

List of Tables

List of Figures

Introduction

Elevation is one of the critical environmental variables that shape biological communities (Janzen, 1967; Sergio & Pedrini, 2007). It follows that the elevational changes wrought by mountains are of great consequence for biogeography, leading to population separation and speciation (Janzen, 1967; McCain, 2004). In the Bolivian Andes, this is manifested first, in rich lowland tropical forests that, second, ascend and transition into the high elevation (ca. 4500 m) Altiplano. Ascending the Andes, there are serially repeated mountain ranges and valleys cutting north to south across the elevational gradient. These result in a pattern that makes the Eastern slope of the Andes a hotbed for speciation.

As a result, Bolivia has extremely high biodiversity (Anderson, 1997), in part also due to its highly variable geology (e.g., Ibisch et al., 1995). This results in a large number of ecoregions and, as such, Bolivia is home to much endemism, with ca. 2402 endemic plant species (Moraes et al., 2018), and 16 endemic mammal species, including *Akodon siberiae* (Anderson, 1997). Animals adapt to their environment whether that be in one distinct biome or in an area of intermediate habitats or merging biomes; these regions are crucial for biodiversity. For small mammals, these transitional habitats show a higher species richness than low or high elevational extremes, and the mid-elevations (700-1500 m) reach a maximum species richness (McCain, 2004). Some mammal species' ranges likely are restricted by higher elevations due to harsher environmental regimes at these elevations, such as extreme changes in temperature, while other species have adapted to the high elevation. The transition zones from sub-tropical and tropical forests to Altiplano, known as the forested "Yungas" (named after the region and province of

1

Yungas in the department of La Paz) and the grassy punas are essential habitat for some mammal species (McCain, 2004; Patterson et al., 1998).

High elevations impose a variety of ecological restrictions and physiological demands on all organisms (Janzen, 1967; McCain, 2004). Limiting factors associated with increasing elevation include: greater daily and seasonal temperature variations, increased rainfall and humidity, and lower partial pressure of oxygen. Together, these factors tend to restrict habitat availability and food resources relative to lower elevations. Importantly, the adaptations enabling mammals to survive the harsh higher elevation climates can be the very characters that fundamentally restrict them to those same habitats (Janzen, 1967; McCain, 2004; Galbreath et al., 2009). As species adapt to the high elevation habitats, they may therefore become less adapted to lower elevation environments (Janzen, 1967; McCain, 2004; Patterson et al., 1998).

The drastic geological and biological transition that occurs from Amazonian or subtropical forests to the Altiplano has been of interest for many years (e.g., Patterson et al., 1998). The rise to the Altiplano is not a smooth, continuous transition but rather is interrupted by numerous mountain ranges and valleys. The north–south oriented valleys and mountain ranges crossing the east–west elevational cline represent another obstacle to animal and plant populations' ability to disperse and maintain connected populations.

Akodon is the one of the most species-rich genera in the class Mammalia, with 39 currently recognized species (Pardiñas et al, 2015; Burgin et al, 2018). *Akodon* is in the family Cricetidae, the second largest mammal family, with over 600 species, including Old and New World rats, mice, hamsters, and lemmings. Within Cricetidae, the

subfamily Sigmodontinae, one of the New World rats and mice groups, contains almost 400 species. The basal radiation of these sigmodontines began between 9.6 to 12 mya (D'Elia, 2003; Pardiñas et al., 2015); well before the Panama land bridge was fully completed. Where in the Americas this radiation began remains in question, but once in South America, it underwent an enormous taxonomic radiation event. Sigmodontinae encompasses several tribes, including the Akodontini, which is composed of over 100 species in 19 genera. It is believed that the Akodontini radiated into these numerous taxa near the Andes mountains (Reig, 1987), although there also is some evidence that the tribe may have in contrast originated in the Argentinian lowlands (Pardiñas, 2015). Regardless of their putative origin and radiation, the genus *Akodon* is estimated to have originated around 2.5 mya (Leite et al, 2014). The most recent Andean uplift, between 11 to 6 mya (Evenstar et al., 2015), provided a broad range of habitats for *Akodon* to settle: the genus ranges throughout most of South America, albeit with only one species in the Amazon basin (Pardiñas et al, 2015). *Akodon*, the type genus of Akodontini, includes the focal species of the present study, *Akodon siberiae*, described by Philip Myers and James L. Patton in 1989. Like other *Akodon* species, it is an inconspicuous, small, dark brown mouse. Many *Akodon* species, and indeed other species in Akodontini, share numerous similarities in external and internal morphological characteristics. These similarities result in the requirement of close inspection of the animals to accurately differentiate and correctly identify them to species. *Akodon siberiae* is believed to be insectivorous, like most other *Akodon* species, although it may be more omnivorous (Myers & Patton, 1989). The geographic range of *A. siberiae* encompasses a small region that extends from

3

ca. 1,800 to ca. 3,100 meters above sea level (masl) on the eastern slopes of the Andes (Roach & Naylor, 2018). It is known to occur in Parque Nacional Amboró, and the neighboring Parque Nacional Carrasco, although most of the existing specimens have been collected near Mt. Siberia (17º51'S, 64º40'W, 2800 m), for which it is named (Anderson, 1997).

Morphology

Morphology has been used to study and determine species identity since the beginning of evolutionary studies of the family Cricetidae (Thomas, 1918). Analyses of external and internal morphology have been the standard tools used to understand rodent taxonomy and systematics (Carleton & Musser, 1989; Voss, 1988). In addition to standard external measurements and qualitative features, in this study I undertook a morphometric analysis of cranial measurements, as shown in Fig. 1 (after Alvarado-Serrano & D'Elía, 2013). Cranial anatomy often is informative of species biology, and dentition (Fig. 2) can inform as to diet and behavior (Carleton &Musser, 1989); both features are character rich and of high value in distinguishing among mammalian species.

Other *Akodon* species with geographic distributions that overlap *A. siberiae*'s small geographic range include *A. mimus*, *A. dayi*, and *A. varius*. The initial description of *A. siberiae* is sufficient in detail to allow distinction from *A. dayi*, and *A. varius* (Myers & Patton, 1989).

However, both *A. mimus*, and superficially, *A. varius* exhibit sufficient morphological variability as to be mistaken for other *Akodon* species, including *A. siberiae*. Features that cause confusion with respect to *A. siberiae* are primarily external: the large total body

length for an *Akodon*, and predominantly dark brown agouti hair with buff tips. When examining skulls, their general shape is similar until a closer examination is undertaken, as this study illustrates.

Genetics

The mitochondrial gene cytochrome b has been commonly used in the study of mammal species relationships (e.g., Smith & Patton, 1991, 1993; Bradley & Baker, 2001; Baker and Bradley, 2006), leading to an extensive database of species for which comparative sequence data exist. The genetics of species of *Akodon* has been investigated in previous studies, and has been a helpful tool in studying relationships, and identifying and describing species (Smith & Patton, 1991; Geise et al, 2001; Jayat et al, 2010). Coyner et al (2013) carried out the largest molecular phylogenetic study of *Akodon.* Given that up to 45 species of *Akodon* have been recognized at any one time, they have been assembled into groups of more closely related species to facilitate elucidation of relationships and taxonomy. Coyner et al (2013) attempted to resolve relationships among *Akodon* species groups using the mitochondrial cytochrome b gene (Fig. 3), as well as the nuclear dentin matrix protein 1 and the nuclear intron thyrotropin. In that study, the relationship of *A. siberiae* and *A. budini* within the aerosus group was supported but not confirmed (Coyner et al., 2013). Since that study, others have used some of the available *Akodon* sequences and generated novel sequence data, but none have focused on the genus *Akodon* itself (Upham, 2019). In this study, I further broadened the phylogenetic analyses of *Akodon* by examining the intrageneric relationships in *Akodon* using all currently available mitochondrial cytochrome b

sequences in conjunction with a targeted morphological analysis of the same species focusing on *Akodon siberiae* and its closely related congeners.

Ecological Niche Modeling

Ecological niche models are a useful tool for predicting where a species might occur (Busby, 1986; Franklin, 1995; Anderson et al., 2002; Sillero, 2011). The method uses environmental variables and cross-references them with known localities where a target species of interest occurs or has occurred, calculating the contribution of each variable to occurrence data. The software then extrapolates the probability of occurrence throughout a region based on similarity in parameters under consideration (temperature and moisture profiles, solar radiation, soils, forest cover, etc.). These models can be useful for various reasons. They can inform where field work can be done when trying to find a species, help understand the environmental parameters that define a species' range and borders, and compare the current range with past or future occurrences.

Here, I examined morphological variation in *A. siberiae* and morphologically similar congeners. In addition, I conducted an investigation into genetic relationships and current habitat of areas of potential occurrence that can be effective in understanding this species. My premise was that a comparison of *A. siberiae* specimens from different but nearby areas, and to closely related species (morphologically and phylogenetically), and using this information in conjunction with an estimation of *A. siberiae*'s habitable areas, would provide insights into the effect of variation in elevation on speciation and morphological variation in the eastern Andes.

<div align="center">

Materials and Methods

</div>

Specimen collection

Specimens were collected in various sites of differing elevations near the town of

Comarapa, bordering Amboró National Park, in the department of Santa Cruz, Bolivia

(Fig. 4). We sampled three sites using standard trapping and collecting methods (Voss &

Emmons, 1996). Sampling was undertaken with permission of private landowners and,

on municipal property, with city permits. The study complied with the American Society

of Mammalogists' guidelines (Sikes et al. 2016).

Collections took place from mid-April to early May 2015. During this time period

the rainy season is ending and transitioning to the dry season. Sampled habitats included

grasslands, subtropical forests, cloud forests, farmland, and seasonally dry shrub land.

The sites where *A. siberiae* was collected were within the Laguna Verde Comarapa City

Park at locations near the Laguna Verde lake, an adjacent cloud forest, and patches of

alpine grass. Two other sampled sites were located south of Comarapa and consisted of

farmland that included dry shrub land and patches of forest but no *A. siberiae* specimens

were collected at these sites.

The latitude, longitude, and elevation, of specific site locations are listed in Table

1. Each site was sampled using 252 Sherman live-traps, 20 snap traps, and 4 Tomahawk

live capture traps. Sherman traps were set in groups of between 30 and 60 (depending on

terrain), in lines of 10, separated by 10 m each. Snap traps were spread evenly among the

trap sites. Traps were set for periods of 6 days, with one day of travel back to Comarapa

to resupply between trapping periods. Peanut butter mixed with oats was used as bait.

Traps were left open 24 hours a day and checked in the mornings. Insulation was not

placed in traps due to the considerable rainfall during the study period. Captured

individuals were identified to species, sex, and approximate age. Specimens were euthanized by thoracic compression, according to ASM Guidelines (Sikes et al., 2016). Specimens were taken to the Museo de Historia Natural Noel Kempff Mercado (MNKM) to be cleaned and museum study skins prepared. Skeletons were cleaned using dermestid beetles. Specimens were accessioned at the MNKM.

 Morphology

To analyze morphological characters and obtain measurements of additional *A. siberiae* individuals, I obtained specimens on loan from the American Museum of Natural History. Specimens of other species of *Akodon* (*A. mimus*, *A. varius*, and *A. dayi*) were measured and compared to my specimens of *A. siberiae*. Samples of these three additional species were obtained from the Colección Boliviana de Fauna (La Paz, Bolivia), Museo de Historia Natural Alcide d'Orbigny (Cochabamba, Bolivia), and The Field Museum (Chicago). *Akodon budini*, the species most closely related to *A. siberiae*, was not included in the comparison because, although they are strikingly similar, their distributions are separated by 250 km and two rivers: the Río Grande and Río Parapetí.

Specimens of *A. siberiae* (Fig. 5) collected as part of this study were compared with previously collected specimens, including the holotype, as well as with *A. mimus*, which is morphologically very similar, to help assess differences among the two taxa. Presence, placement, and length of vibrissae were compared. Stomach contents were checked for arthropod and plant material. External measurements taken included: total length, tail length, ear length, hind foot length, and length of head and body (Table 2). Hair color was compared from the dorsal, ventral, and lateral areas of the body. Cranial

measurements recorded (n = 27) were based on the initial description of *A. siberiae* (Myers & Patton, 1989) and the Mammals of Bolivia (Anderson, 1997) these are listed in Table 3 and 4. Principal component analysis was carried out on the quantitative characters to assess morphological variability within and among *A. siberiae* were *A. mimus*, *A. varius*, and *A. dayi*. A qualitative comparison of morphological characters was not conducted on *A. varius* or *A. dayi* because species identification among them is less difficult. Following a principal component analysis, the two measurements that have the highest loading values—those with the greatest contribution to principal components 1 and 2—can be used in the future as a guide when discriminating between the species included in the analysis.

Genetics

Following the genetic methods of Coyner et al. (2013), I analyzed mitochondrial cytochrome b genes of 17 *A.siberiae* specimens and constructed a phylogenetic tree (Smith & Patton, 1991). Cytochrome b sequences of two *A. siberiae* specimens available in GenBank (accession numbers U03548 and AY277430) also were included in the analysis. Muscle tissue was extracted from the specimens at time of death or, if specimens were kept in alcohol, DNA was extracted from muscle tissue; the skull was removed at the same time. Tissues were kept in alcohol at -80º C.

DNA extraction

Genetic methods followed QIAGEN (Germantown, Maryland) QIAquick protocols, using a DNeasy Blood and Tissue kit. Approximately 2 grams of skeletal muscle or brain was extracted from each individual. Tissue samples were triturated using a scalpel and resulting tissue placed into a solution containing 20 mL Proteinase K and

180 mL ATL buffer. The solution was vortexed until thoroughly mixed and left for 12

hours in a 57º C water bath. The DNA then went through a filtration and elution process:

following the water bath, the solution was vortexed, 200 µL of AL Buffer were added,

and the resulting mix left in a 56º C bath for 10 minutes. The solution was then pipetted

into a DNeasy mini spin column and placed in a collection tube. Samples were then

centrifuged for one minute; the flow through and collection tube were discarded. The

spin column was placed in a new collection tube. 500 µL of AW1 Buffer was added to a

spin tube and centrifuged for 3 minutes. The flow through and collection tube were

discarded and the spin column placed in a new collection tube. 500 µL of AW2 Buffer

were added to the spin tube, which was centrifuged for 3 minutes. The flow through and

collection tube were then discarded. The spin tube was then placed in a 1.5 mL centrifuge

tube. 125 µL of AE Buffer were added to the spin column to release DNA from the spin

tube filter. The flow through was saved as the first round of extracted DNA. 50 µL of AE

Buffer was added to the mini spin tube for the second round of extracted DNA.

PCR amplification

The filtered DNA was amplified by polymerase chain reaction (PCR). The

akodontine cytochrome b sequence is approximately 1140 base pairs long (Smith &

Patton, 1991). External primers used included MVZ05 and MVZ 14 (Smith & Patton,

1991). To ensure higher accuracy for Sanger sequencing, overlapping internal primers

MVZ 26 and MVZ 39 were also used in separate runs (Smith & Patton, 1993). A Master

Mix of each primer was prepared consisting of 66 µL H_2O, 3 µL of forward primer, and 3

µL reverse primer. 22 µL of Master Mix and 3 µL of amplified DNA were added to a

microcentrifuge tube containing PCR beads (GE Pittsburgh). The solution underwent

cyclical temperature change regimen in a thermocycler. Amplifications were performed using the following thermal profile: initial denaturation at 95°C for 3 min, 35 cycles of 95°C for 30 s, 48–55°C for 50 s, and 72°C for 1 min, and a final elongation at 72° C for 10 min. Sequences that were low in purity and missing large sections were not used in the final analysis discussed below, resulting in the second phylogenetic tree.

PCR product purification

The PCR reaction product was purified to remove non-DNA constituents and placed into a spin column and collection tube. 125 µL of PB Buffer were added to the solution and mixed. The solution was then centrifuged for 1 minute. The flow through was discarded. To wash, 750 µL of PE Buffer was added and the solution centrifuged for 1 minute, discarding the flow through and collection tube. The spin tube was then placed in a 1.5 mL centrifuge tube and 50 µL EB Buffer added to the spin tube and centrifuged for 1 minute. That product was sequenced by the Oregon Health and Science University's DNA Services Core.

Phylogenetic Analysis

A molecular phylogenetic tree (Fig. 6) based on the 1140 base pair cytochrome b sequences was constructed using 17 of the 54 *A. siberiae* specimens collected, as well as 349 additional *Akodon* specimens, including 37 *Akodon* and 4 other akodontine species, whose sequences were downloaded from Genbank. *Oxymycteris paramensis* was designated as the outgroup, as it is a species within the subfamily. Sequences were aligned using ClustalW on the CyberInfrastructure for Phylogenetic RESearch (CIPRES) server (Miller et al., 2010). A phylogenetic tree was generated using the Maximum

Likelihood algorithm as implemented in RAxML-HPC v.8 (Stamatakis, 2014) on the

CIPRES server, and the General Time Reversible model of evolution with Gamma rate

parameter for rate heterogeneity (GTRGAMMA). This model optimizes substitution rates

across the gene and simultaneously evaluates likelihood values for the resulting tree

(Stamatakis, 2014). As the species in the tree resolved with confidence, and specimens

of each species grouped together, a second tree (Fig. 7) was constructed using one

specimen for each species in order to clarify some of the more complex relationships.

This second tree was generated using the first 801 base pairs of the cytochrome b gene

sequence, as many of the compared sequences were that length.

Ecological niche models

Ecological niche models estimate probability of geographical occurrence of

species based on abiotic ecological variables obtained from the geographic locations of

collected specimens. Ecological variables were downloaded from climond.org (Kriticos

et al, 2012). Thirty-seven variables were used, including: altitude, ecological region,

maximum temperature of the warmest month, precipitation of coldest quarter, etc. A

complete list of variables is provided in Table 5. The data coverage of these variables

range from 1961 to 1990. Using ArcGIS software, these variables were geographically

limited to data from South America. The software used to calculate the environmental

niche model was Maxent (Philips et al., 2006), which runs a maximum entropy model.

The model was run using known *A. siberiae* occurrences based on specimens studied.

These included the 54 specimens collected in this study and 30 specimens collected in

previous studies about 30 km west of Comarapa, along the main highway (see Appendix

I, Specimens examined). Using these localities, Maxent takes the values of the variables

12

at those points, determines if those variables are correlated to localities, and extrapolates and predicts where *A. siberiae* could occur. Settings were set according to Phillips et al. (2006) and Young et al. (2011). Settings for the runs were set to a replicated run type of bootstrap. Response curves for the variables were created and jackknives carried out to measure variable importance. A random seed of 20 percent of data points was used, with 10 replicates in each run and maximum iterations set to 5000. For the first run, all ecological variables were used; for the next run, only variables that resulted in more than one percent contribution to the model were used. For subsequent runs, the least contributing variable was removed for the following run; this process was iteratively repeated until only one variable was used. To determine which model was the most informative, we used the run with the highest Area Under Curve for the calculated Sensitivity vs. Specificity, which measures the accuracy of the prediction of occurrence. The model was then edited in the geostatistical program, ArcGIS.

Results

I sampled a total of 7501 trap nights, resulting in the capture of 93 small mammals (1.3% trap success). Captures included: one White–bellied Slender Mouse opossum,
Marmosops noctivagus (Tschudi, 1845); 11 Buff–bellied Fat–tailed Mouse Opossums, *Thylamys venustus* Thomas, 1902; 54 Cochabamba Grass Mice, *A. siberiae*; 11 Paraguayan Bolo Mice, *Necromys lenguarum* (Thomas, 1898); 15 Pale Leaf-eared Mice *Graomys domorum* (Thomas, 1902); one Light–footed Rice Rat, *Nephelomys levipes* (Thomas, 1902); and one Common Yellow-toothed Cavy, *Galea musteloides* (Meyen, 1832); A Molina's Hog–nosed Skunk, *Conepatus chinga* (Molina, 1782), was captured in

a Tomahawk trap in Site 12 and released. Between the Laguna Verde and site 12, we also observed a troupe of Black Howler Monkeys, *Alouatta caraya* (Humboldt, 1812).

A morphological comparison among the holotype, previously collected specimens of *A. siberiae*, and specimens collected in Comarapa showed scant morphological variation. The skull and mandible of an *A. siberiae* specimen is shown in Fig. 8. The fur and hair morphology of species can be helpful in species identification. The fur of the Comarapa specimens is similar to that of specimens described in the original description. There are two hair types on the dorsal side, one agouti and one all Blackish Neutral Gray (Color 82 of Naturalist's Color Guide; Smithe, 1975). The agouti hairs on the dorsal side have a Blackish Neutral Gray base, a Yellow Ochre (Color 123C) band, and a dark tip. The hairs of the head have a total length of 6-10 mm, increasing to an average of 11 mm at the mid dorsum, and then decreasing to an average of 10 mm at the rump. The dorsal agouti hairs have a Yellow Ochre band of 1 mm, and the dark tip is 0.5 – 1 mm. The venter does not contain any black hairs, or dark tips on the hairs. The Yellow Ochre bands change to Buff (Color 124) and increases to an average of 2 mm, as the total length of the hairs becomes 9 mm. The pattern changes gradually from the dorsum to the ventrum. The overall effect gives the members of this species a subdued countershading pattern, appearing dark brown dorsally, and light tan ventrally. Skin color on the pinnae is dark externally and lighter internally, almost completely dark in holotype and previously collected specimens. Pinna shape is rounded, with the hair on the pinnae brown to tan and sparser than on the holotype. No eye rings were present in any specimen examined. The skin of eyelid is dark brown. Mystacial and a short submental vibrissa present, and occasionally one superciliary vibrissa; this is more than the

holotype's vibrissae, which only has mystacial vibrissae, although other specimens collected by Myers and Patton (1989) sometimes had submental vibrissae. The tail is softly bicolored; the dorsal side is mostly medium brown, and the ventral side hair is a little lighter. Tail length is less than head-body length: specimens collected in this study have an average tail length of 46% of the total body length. Tail hairs are short and brown. Tail scutes are parallel. Skin color on the toes is a little lighter than that on the feet. Hair on the feet is sparse, and barely extends past the claws. Stomach contents of three specimens revealed an omnivorous diet: both vegetation and insect fragments were found, similar to most *Akodon* species. In addition to the peanut butter and oat bait, some vegetable material, likely grass leaves, and insect antennae from undetermined species were present.

Cranial differences between *A. siberiae* and *A. mimus* are shown in Figs. 9 and 10. The incisive foramina of *A. siberiae* extend further posteriorly than those of *A. mimus*, past the first mesoflexus of the first molar; *A. siberiae* also has a thinner interorbital breadth. Although not shown quantitatively on the rostrum width measurements, the incisive root bulb ampulla of *A. siberiae* extends noticeably laterally. The post-palatal pits are a greater distance posterior from the palatine foramina in *A. siberiae*. The sphenopalatine vacuity is wider in *A. siberiae*. The carotid canal is smaller in *A. siberiae*. The petrotympanic groove is smaller in *A. siberiae*.

The geographic range of *A. mimus* overlaps completely the small range of *A. siberiae*, and distinguishing between these two species is particularly difficult. In the description of *A. siberiae* (Myers and Patton, 1989), the authors noted differences with respect to *A. mimus* to assist in identification. Unfortunately, in that study, the dentition

of all specimens was too worn to distinguish many dental characters. Specimens

collected in the present study had easily discernible dental characters, and we were able

to undertake interspecific dental character comparisons (Fig. 11). The anteromedian

flexus constituted the most notable difference, being present in *A. siberiae* and absent in

A. mimus. All other flexa (paraflexus, mesoflexus, and hypoflexus) on *A. siberiae* are

deeper or present where they may be shallow or absent in *A. mimus* specimens. These

features tend to disappear if wear is extensive, so this may potentially be construed as a

product of differential wear; however, it appears to constitute a genuine distinction

between the two species. This is more evident on *A. mimus* specimens that had minor

wear, revealing that these dental characters remain shallow or absent in this species. The

zygomatic plate of *A. siberiae* extends straight superiorly from the base. It then can have

an angle or short curve, meeting the zygomatic arch. The zygomatic plate of *A. mimus* is

"microxine," which is to say thin and slanted at a reverse angle its entire length, as is

present in *A. mimus* and *Neomicroxus* species, as shown in Fig. 12.

A comparison of the measurements of *A. siberiae* and *A. mimus* is provided in

Tables 2, 3, and 4. All their values overlap, reinforcing the difficulty in differentiating

the two species. However, the principal component analysis (PCA), shown in Fig. 13,

revealed that it is possible to determine taxonomic identity of the two species based on

cranial measurements. The variable loading values of the PCA are listed in the loading

matrix (Table 6). The measurements that had the highest loading values and thus

affected the principal components 1 and 2 were condylo-incisive length and rostrum

length, respectively. The condylo-incisive length of *A. siberiae* averaged of 24.97 mm,

range 23.46 - 26.62 mm; that of *A. mimus* is 23.63 mm (21.14 - 25.18). Rostrum length

of *A. siberiae* is 9.85 mm, (9.06 to 10.5). That of *A. mimus* is 10.0, (8.04 - 11.06). The

eigenvalues in Table 7 show that PC1 had a larger value than PC2, 9.2 v. 2.9. PC1 had a

percent contribution of 36.8%, and PC2, 11.8%. Fig. 14 shows the eigenvalues of all

calculated principal components, with the percent contribution illustrated by the curve.

The two-dimensional relationship between the principal components 1 and 2 based on

the measured variables is shown in Fig. 14. However, the raw measurement values and

data points on the PCA (Fig. 13) may be misleading when used to understand

evolutionary relationships. The Loading plot, showing the variables used in the PCA and

the relationship of each variable to PC1 and PC2 is shown in Fig. 15. The grouping of

the *A. siberiae* data points (Fig. 13) in multivariate space is tightly pressed to the cloud

of points representing *A. mimus*, and more distant to *A. varius*, with which *A. siberiae* is

more closely related based on the phylogenetic tree. This emphasizes the difficulty of

previous species identification, and the need for multiple independent data sources.

A phylogenetic tree based on cytochrome b sequences was constructed using 17

of the 54 *A. siberiae* specimens collected, as well as 349 other *Akodon* specimens of 35

species and 4 other Akodontini species whose sequences were downloaded from

GenBank (Fig. 6). The species, specimens used, localities, and accession numbers are

listed in Appendix I. The 19 specimens of *A. siberiae* include 17 from the present

collection and two from Genbank. These jointly form a monophyletic clade.

A second tree, constructed using the first 801 bp of cytochrome b (Fig. 7),

includes three of the *A. siberiae* specimens collected in this study and the two previously

collected. The five major species groups described by Coyner et al. (2013) and Jayat et al. (2010), and were resolved in this work as well. A notable difference is that, in this study, *A. mimus* was placed in the *aerosus* group. Coyner et al. (2013) were unable to unequivocably resolve the relationships of that species. In the tree resulting from the present data, *A. mimus* was placed outside the clade formed by *A. siberiae* and *A. budini*, within the *aerosus* group. The *varius* group does not remain in the *aerosus* group in this tree. In addition, the *cursor* group, while maintaining its integrity, differs somewhat from that of Coyner et al. (2013) with respect to interspecific relationships among species within the group. The *boliviensis* and *dolores* groups remain unchanged from this study's comprehensive tree (Fig 6).

The ecological niche model (Fig. 16) shows where *A. siberiae* could occur based on the 37 environmental variables used in this study (Table 5). The seventh run of the model had the largest Area Under Curve (AUC), hence the most predictive power. This model had a Mean AUC 0.995 (Fig. 17). That run used three environmental variables: elevation, precipitation during warmest quarter, and temperature seasonality (i.e., annual range in temperature). Elevation contributed 56.5% to the model; precipitation during warmest quarter, 22.9%; and temperature 20.6%. The elevation for which the model predicted 0.7-1 probability of occurrence was ca. 1750 - 3000 masl. The values of precipitation where the model predicted 0.7-1 probability of occurrence were ca. 291 - 1100 mm (Fig. 18). Finally, the 0.7-1 probability of occurrence all resided at lower than 0.01 seasonality of temperature; this is a dimensionless index which ranges globally from 0 to 0.08.

<div align="center">**Discussion**</div>

Genetics

      The phylogenetic trees resulting from the analysis of the sequences derived from this study confirms the assessment of relationships made by Coyner et al. (2013) that *A. siberiae* is the sister species to *A. budini*. Further, Coyner et al. (2013) indicated that *A. siberiae* and *A. budini* are members of the *A. aerosus* species group of *Akodon*, although they concluded that further study was needed. Here, we confirm that *A. siberiae* and *A. budini* indeed reside in the *aerosus* group, as additional specimens of *A. siberiae* cemented their position within that group. Coyner et al. (2013) used 176 cytochrome b sequences, whereas 356 sequences were used in the present study. The larger sample size in my study was possible because of the greater number of sequences deposited in GenBank since the Coyner et al. (2013) study, but also because Coyner et al. restricted themselves to sequences 1000 bp or longer in length. Sequences generated for the present study were all shorter than 1000 bp. Accordingly, for one tree, all available GenBank sequences were used, regardless of size. Species present in Coyner et al. (2013), but not in this study, include one specimen of each of the following: *A. surdus*, *A. affinis*, and *A. orientalis*.

      The present study found five species groups, the four as found in Coyner et al. (2013): *aerosus*, *boliviensis*, *cursor*, and *varius* groups, and including the dolores group, as discussed by Jayat et al. (2010). The *aerosus* group contains *A. aerosus*, *A. affinis*, *A. albiventer*, *A. baliolus*, *A. budini*, *A. glaucinus*, *A. mollis*, *A. orophilus A. siberiae*, *A. surdus*, *A. tartareus*, *A. torques*, and *A. varius*. Coyner et al. (2013) included *A. varius* and *A. simulator* in the *aerosus* group, but other authors disagreed with that assignment

<div align="center">19</div>

(Pardiñas et al, 2015). The larger tree constructed here agrees with Coyner et al. (2013) that *A. varius* and *A. simulator* belong in the *aerosus* clade. *Akodon mimus* could belong in the *dolores* species group. There were several polytomies in the cytochrome b phylogenetic tree of Coyner et al (2013), as shown in Fig. 3. Polytomies are sections of a phylogenetic tree in which branching order of different taxa or clades is unresolved, resulting in the representation of many branches simultaneously originating from a single node due to uncertainties in the phylogenetic analysis. In the Coyner et al. (2013) study, some of these polytomies were resolved with a tree generated from data of cytochrome b concatenated with sequences of the dentin matrix protein gene and the thyrotropin intron. This multiple gene tree could not make use of all the same specimens, as fewer of them had all three genes sequenced. As a result, their concatenated tree only included 80 specimens of 25 species. The cytochrome b tree used in our study matches the resolution of the Coyner et al. (2013) concatenated tree and further identifies relationships of taxa not included in that study: *A. orophilus* is in a clade with *A. siberiae* and *A. budini*, and *A. torques* appears to be sister to *A. aerosus*.

In the phylogenetic tree constructed with the first 801 bp of cytochrome b (Fig. 7) most relationships were unchanged. However, there is a change in the phylogenetic association of *A. mimus*, now located in the *aerosus* group. This result conflicts with other genetic studies of *Akodon*, including the other tree generated in this study (Fig. 6), and thereby presents an interesting issue. A possible reason for this shift could be that the first 801 bp of the cytochrome b are correlated with the similarities between *A. mimus* and *A. siberiae* described in this study, as the gene is a component of the electrochemical proton gradient that eventually results in the synthesis of adenosine triphosphate. It is

therefore potentially reasonable to hypothesize that the sister taxon relationship as expressed by cytochrome b is associated with the physiological constraints of residing within identical habitats. Since the change of the other microxine species, *A. bogotensis* and *A. latebricola*, into the new genera *Neomicroxus*, *A. mimus* was left with uncertain placement among *Akodon*. It could be a reasonable to place *A. mimus* in the *aerosus* group, as other species in the *aerosus* group do share morphological characteristics with *A. mimus*. Its microxine zygomatic plate would then be a novel character within this group. As no other study has produced this relationship, it conversely could be more likely that this result is not representative of true relationships. Indeed, the low bootstrap values do not give this relationship strong support, and this has not been the relationship of *A. mimus* in previous work (Coyner et al., 2013). Another change seen in this tree is that the *varius* group was removed from the *aerosus* group. This difference reflects the current debate as to the *varius* group's inclusion in the *aerosus* group or its independence (Coyner et al., 2013; Pardiñas et al., 2015).

Morphology

Investigating the differences between *A. siberiae* and *A. mimus* is critical to future identification and taxonomic work. Other *Akodon* species with overlapping ranges can have similar to identical fur patterns as do *A. varius* and *A. mimus*. Although *A. mimus* bears much resemblance to *A. siberiae*, the phylogenetic analysis demonstrated in the first tree of this study and other studies that this general similarity is due to convergent evolution within the genus. The phylogenetic tree established that similarities such as general size and color evolved separately within *Akodon*.

Akodon mimus ranges from Yungas to high elevation grasslands and overlaps the

distribution of *A. siberiae*. Both *A. siberiae* and *A. mimus* are omnivorous. Because

sharper molars often indicate an insectivorous diet, and flatter molars indicate a more

herbivorous diet (Martin et al., 2016), it may be that *A. siberiae* has a diet that is more

dependent on insects, whereas *A. mimus* may have a more vegetable dependent diet in the

higher elevations, where fewer insects occur (Olson, 1994).

Ecological niche model

Predictably, the ecological niche model shows areas of high probability of

occurrence at elevations similar to those in which *A. siberiae* is known to occur. The

model also showed where one might have a higher probability of finding *A. siberiae*. The

model shows probability of occurrence, with 0 being no probability of occurrence and 1

being the highest probability of occurrence. The overall area does roughly resemble the

range currently estimated for *A. siberiae* by Roach and Naylor (2018). However, the

predicted area with a probability of occurrence value greater than 0.7 is considerably

smaller than this range. This emphasizes the vulnerability of the species to potential

disturbance events. Despite the fact that the ENM model is based on actual specimen

data, localities where other researchers have collected *A. siberiae* are in areas with only a

0.2 – 0.35 probability of occurrence. The reason for this disparity is unclear, although

with more documented specimen localities, the model improves in predictive capability.

In certain localities, the habitat of *A. siberiae* is cloud forest, where precipitation can be

quite high. Since the variable of precipitation that produced the best model was during

the warmest month, this implies that the importance of this ecological character is

connected to plant growth. Because the diet of *A. siberiae* consists of some grasses and insects, this connection could be direct or indirect, although strong and thus potentially indicative of a specific dietary requirement. There are areas of high probability of occurrence on the western edge of the Carrasco National Park and south of Amboró National Park. These areas currently have little habitat destruction. There is also an area of high probability to the west of, and near, the city of Cochabamba (from which *A. siberiae* gets its common name). The possibility of expansion to those areas is, however, unlikely, because species with such restricted ranges are likely to inhabit a very specific habitat (Roach & Naylor, 2018). *Akodon siberiae* has been found in mostly undisturbed cloud forests and neighboring alpine meadows and grasslands and is not believed to occur, or even be able to persist, in modified habitat (Pardiñas 2015). There were no A. siberiae specimens collected in the farm or ranch lands in this study. Indeed, major threats to this species include destruction of cloud forest habitat for cattle pasture (Roach & Naylor, 2018). A highway already transects its range, and further fragmentation of the habitat can easily ensue. The IUCN lists *A. siberiae* as Near Threatened, with a decreasing population trend (Roach & Naylor, 2018) and there is a need to prevent further destruction of the species' habitat (Roach & Naylor, 2018).

The ecological niche model does not, however, take into account several factors. Direct interactions with other species are not entered in the model, including negative interactions such as predation and competition. Conversely, any positive interactions with plant or insect species that are prey to *A. siberiae* likewise are not used in making the determination of where that species could occur.

Based on the phylogenetic tree, the species most closely related to *A. siberiae* include *A. budini*, *A. orophilus*, and *A. aerosus*, and perhaps *A. mimus*. These all reside in similar forested Yungas habitats, with *A. aerosus* ranging from the immediately neighboring mountains and valleys to the north of *A. siberiae* to Ecuador; *A. budini* around 250 km to the south; and *A. orophilus* found in the Andes' eastern slopes of Northern Peru. The ranges of other species in the *aerosus* group continue this trend through most of the Andes. From these data, we can infer that a common ancestor of *A. siberiae* and *A. budini* may have originated at mid-elevations of central Bolivia to Northern Argentina, likely by chance dispersal of one or the other taxa across the Rio Grande, although vicariance as a result of recent changes in the flow of the Río Grande (Plotzki et al., 2013) cannot be excluded. *Akodon mimus* elevational range spans from about 2,000 m to 3,700 m, whereas *A. siberiae* spans from 1,800 m to 3,100 m, though *A. siberiae*'s range is much smaller than that of *A. mimus*. This study provides evidence that the phylogenetically divergent *A. mimus* convergently evolved a morphology similar to that of species in the *aerosus* group (particularly *A. siberiae*), which live in similar Yungas habitats. Alternatively, *A. mimus* could be nestled in the *aerosus* group, and more genetic research must be done to clarify its relationships, including using other genetic sequences. The morphology that *A. siberiae* and *A. mimus* share could have been selected for by similar evolutionary pressures, e.g. diet for dentocranial morphology and environmental pressures for general body size and coloration. Or they share this evolutionary history as species within the *aerosus* group. This, along with the ecological niche model that shows elevation as the most important factor for the occurrence of *A. siberiae*, demonstrates that orogenic processes leading to mountain range building with

24

intervening valleys, along with shifting river courses, indeed served as a barrier to movement and consequently as a catalyst to mammalian speciation in the Andes.

Conclusion

This study has illuminated different aspects of the biology of *A. siberiae*. From the morphological analysis, I infer that the morphologies that *A. siberiae*, *A. mimus*, *A. varius*, and *A. budini* share may be based in the Yungas habitat, and perhaps their place in the ecosystem. In particular, *A. siberiae* and *A. mimus* are almost indistinguishable morphologically, save for noted examples, such as the thin slanted zygomatic plate of *A. mimus* and the more defined dentition of *A. siberiae*. The genetic relationships of *A. siberiae* within the genus have been confirmed that *A. siberiae* falls within *aerosus* species group, the members of which have evolved to occupy the Yungas habitats along the eastern foothills of the Andes. The areas from which these species' morphologies adapted, may have indeed separated them. The geological and elevational variation and the larger rivers Río Grande and Río Parapetí may also have served to separate the ancestor of *A. siberiae* and *A. budini* resulting in their speciation. The ecological niche model shows that *A. siberiae* can only thrive in the small regions forested with moist cloud forest, undisturbed by humans, in certain areas around the cities of Cochabamba and Comarapa. These pockets, within and outside of protected parks, are in danger of destruction. The future of the species therefore depends on enforced protection of those areas.

Tables

Table 1. Collection site locations. Note, only sites 12, 13, 14, and 15 were in Laguna Verde, where *Akodon siberiae* specimens were collected.

Collection Site	Latitude (decimal degrees)	Longitude (decimal degrees)	Elevation (masl)
1	-18.0178	-64.4557	1646
2	-18.0208	-64.460	1749
4	-18.0269	-64.4656	1942
5	-17.5823	-64.2622	1702
6	-17.5825	-64.2627	1712
7	-17.9737	-64.4389	1774
8	-17.9703	-64.4341	1663
9	-17.9707	-64.4352	1665
12	-17.8778	-64.5117	2519
13	-17.8794	-64.5088	2594
14	-17.8729	-64.5107	2707
15	-17.8720	-64.5111	2711

Table 2. External and cranial measurements (in mm unless otherwise stated), used in the Principal Component Analysis.

Total Length
Tail Length
Hind Feet Length
Weight (g)
Head and Body Length
Occipital-nasal Length
Alveolar Length
Length of Rostrum
Breadth of Braincase
Postdental Breadth
Zygomatic Breadth
Interorbital Breadth
Condylo-incisive Length
Breadth of First Molar
Nasal Length
Rostral Width
Orbital Length
Diastema Length
Maxillary Toothrow Length
Incisive Foramina Length
Palatal Bridge Length
Palatine Bone Length
Alveolar Width
Occipital Condyle Width
Basioccipital Length
Mesopterygoid Fossa Length
Mesopterygoid Fossa Width
Zygomatic Plate Breadth
Cranial Depth

Table 3a. Mean, Standard Deviation, Minimum, and Maximum of external and cranial measurements of Akodon siberiae used in the Principal Component Analysis.

Akodon siberiae Measurements N=22	Total Length	Tail Length	Hind Foot Length	Ear Length	Weight	Head-Body Length	Occipito-nasal Length	Alveolar Length of Toothrow	Zygomatic Breadth	Breadth of M1	Interorbital Breadth	Condylo-incisive Length	Nasal Length	Rostral Width	Orbital Length	Palatine Bone Length
Mean	192.13	88.88	24.54	17.54	26.29	103.25	27.36	4.79	13.29	1.16	5.17	24.97	10.41	5.1	8.31	1.76
Standard Deviation	9.02	5.8	1.04	2.93	4.79	5.14	0.53	0.29	2.47	0.12	0.2	0.68	0.55	1.14	0.25	0.15
Minimum	178	77	22.5	13	20.8	94	26.08	3.9	2.34	0.99	4.84	23.46	9.26	4.33	7.86	1.46
Maximum	210	98	26	21.5	35.5	114	28.23	5.14	14.56	1.4	5.58	26.62	11.7	10.1	8.82	2.06

Table 4a. Mean, Standard Deviation, Minimum, and Maximum of external and cranial measurements of *Akodon minus* used in the Principal Component Analysis.

Akodon minus Measurements N=44	Total Length	Tail Length	Hind Foot Length	Ear Length	Weight	Head-Body Length	Occipito-nasal Length	Alveolar Length of Toothrow	Zygomatic Breadth	Breadth of M1	Interorbital Breadth	Condylo-incisive Length	Nasal Length	Rostral Width	Orbital Length	Palatine Bone Length
Mean	181.19	90.14	22.30	15.81	19.70	91.05	26.77	4.69	12.75	1.24	5.53	23.63	10.61	4.66	7.63	1.87
Standard Deviation	17.32	12.90	2.43	2.54	4.82	9.37	1.16	0.28	0.89	0.11	0.38	1.05	0.69	0.30	0.40	0.21
Minimum	143	64	13	9	12	67	24.06	4.28	9.88	1.02	4.86	21.14	8.92	4.04	6.66	1.32
Maximum	219	117	29	26	31.50	107	29.88	5.30	14.86	1.48	6.20	25.18	11.74	5.24	8.44	2.26

Table 3b . Mean, Standard Deviation, Minimum, and Maximum of external and cranial measurements of *Akodon siberiae* used in Principal Component Analysis.

Akodon siberiae	Alveolar Width	Occipital Condyle Width	Mastoid Breadth	Basioccipital Length	Mesopterygoid Fossa Length	Length of Rostrum	Breadth of Braincase	Postdental Breadth	Diastema Length	Maxillary Toothrow Length	Palatal Bridge Length	Mesopterygoid Fossa Width	Incisive Foramen Length	Zygomatic Plate Breadth	Cranial Depth
Mean	5.19	6.57	10.84	3.85	4.14	9.85	12.24	3.51	8.05	4.48	3.86	1.66	6.27	2.09	9.58
Standard Deviation	0.48	0.28	0.31	0.33	0.34	0.43	0.34	0.23	4.38	0.78	0.32	0.18	0.39	0.23	0.34
Minimum	3.62	5.75	9.98	3.48	3.45	9.06	11.38	3.11	6.6	1.24	3.26	1.24	5.06	1.63	9.04
Maximum	6	7.06	11.22	4.9	4.7	10.5	12.71	3.96	27.6	4.86	4.36	2.02	6.88	2.68	10.52

Table 4b. Mean, Standard Deviation, Minimum, and Maximum of cranial measurements of *Akodon minus* used in the Principal Component Analysis, continued

Akodon minus	Alveolar Width	Occipital Condyle Width	Mastoid Breadth	Basioccipital Length	Mesopterygoid Fossa Length	Length of Rostrum	Breadth of Braincase	Postdental Breadth	Diastema Length	Maxillary Toothrow Length	Palatal Bridge Length	Mesopterygoid Fossa Width	Incisive Foramen Length	Zygomatic Plate Breadth	Cranial Depth
Mean	5.52	6.42	10.54	3.67	4.10	10.01	11.91	3.63	6.72	4.41	4.10	1.67	5.56	1.82	9.46
Standard Deviation	0.48	0.30	0.42	0.25	0.27	0.67	0.41	0.27	0.61	0.25	0.58	0.18	0.30	0.22	0.67
Minimum	4.10	5.76	9.86	3.24	3.24	8.04	11	3.26	4.22	3.98	2.94	1.36	4.62	1.50	6.52
Maximum	6.50	7.00	11.76	4.44	4.56	11.06	12.56	4.92	7.68	4.86	5.12	2.16	6.00	2.36	10.40

Table 5. Bioclimatic environmental variables used in creating ecological niche models of *Akodon siberiae*.

Variable	Variable description
Bio01	Annual mean temperature (°C)
Bio02	n diurnal temperature range (mean(period max-min)) (°C)
Bio03	Isothermality (Bio02 ÷ Bio07)
Bio04	Temperature seasonality (C of V)
Bio05	Max temperature of warmest week (°C)
Bio06	Min temperature of coldest week (°C)
Bio07	Temperature annual range (Bio05-Bio06) (°C)
Bio08	Mean temperature of wettest quarter (°C)
Bio09	Mean temperature of driest quarter (°C)
Bio10	Mean temperature of warmest quarter (°C)
Bio11	Mean temperature of coldest quarter (°C)
Bio12	Annual precipitation (mm)
Bio13	Precipitation of wettest week (mm)
Bio14	Precipitation of driest week (mm)
Bio15	Precipitation seasonality (C of V)
Bio16	Precipitation of wettest quarter (mm)
Bio17	Precipitation of driest quarter (mm)
Bio18	Precipitation of warmest quarter (mm)
Bio19	Precipitation of coldest quarter (mm)
Bio20	Annual mean radiation (W m^{-2})
Bio21	Highest weekly radiation (W m^{-2})
Bio22	Lowest weekly radiation (W m^{-2}
Bio23	Radiation seasonality (C of V)
Bio24	Radiation of wettest quarter (W m^{-2})
Bio25	Radiation of driest quarter (W m^{-2})
Bio26	Radiation of warmest quarter (W m^{-2})
Bio27	Radiation of coldest quarter (W m^{-2})
Bio28	Annual mean moisture index
Bio29	Highest weekly moisture index

Table 5 continued. Bioclimatic environmental variables used in creating ecological niche models of *Akodon siberiae*.

Bio30	Lowest weekly moisture index
Bio31	Moisture index seasonality (C of V)
Bio32	Mean moisture index of wettest quarter
Bio33	Mean moisture index of driest quarter
Bio34	Mean moisture index of warmest quarter
Bio35	Mean moisture index of coldest quarter
Bio36	Elevation
Bio37	Ecological region

Table 6. The Loading Matrix of the Principal Component Analysis, showing the loading values of each cranial measurement. The measurements with the highest values for principal components 1 and 2 are in bold.

	Principal 1	Principal 2
Condylo-incisive Length	**0.89894**	-0.11640
Alveolar Width	0.80163	0.18669
Mesopterygoid Fossa Width	0.79543	-0.21351
Occipitonasal Length	0.79192	0.26860
Orbital Length	0.77127	-0.35405
Zygomatic Breadth	0.76809	-0.15793
Cranial Depth Length	0.75701	-0.04453
Palatal Bridge Length	0.69937	0.41229
Alveolar Length of Toothrow	0.69194	-0.13623
Postdental Breadth	0.66336	-0.16048
Mesopterygoid Fossa Length	0.64161	0.12791
Mastoid Breadth	0.61329	0.10366
Basioccipital Length	0.61211	-0.15669
Breadth of Braincase	0.61095	-0.07167
Palatine bone Length	0.60421	-0.06342
Rostral Width	0.53700	-0.08771
Breadth of M1	0.51443	-0.17062
Maxillary Toothrow Length	0.44508	-0.01259
Occipital Condyle Width	0.41326	-0.29656
Incisive Foramen Length	0.34627	-0.40129
Length of Rostrum	0.33879	**0.85333**
Nasal Length	0.31141	0.78794
Interorbital Breadth	0.2647	0.80471
Zygomatic Plate Breadth	0.26314	-0.26124
Diastema Length	0.18166	0.04500

Table 7. The eigenvalues and percentage of explained variance of principal components of the PCA.

Number	Eigenvalue	Percent
1	9.2030	36.812
2	2.9463	11.785
3	2.3125	9.250
4	1.4508	5.803
5	1.2969	5.187
6	1.0330	4.132
7	0.9721	3.889
8	0.8268	3.307
9	0.7093	2.837
10	0.6362	2.545
11	0.5332	2.133
12	0.5006	2.002
13	0.4594	1.838
14	0.3640	1.456
15	0.3230	1.292
16	0.2789	1.116
17	0.2435	0.974
18	0.1965	0.786
19	0.1739	0.696
20	0.1693	0.677
21	0.1318	0.527
22	0.0859	0.344
23	0.0724	0.290
24	0.0600	0.240
25	0.0207	0.083

Figures

1.	ONL	15.	BM1
2.	ZB	16.	BPB
3.	IB	17.	LN
4.	BR	18.	BN
5.	LB	19.	BB
6.	HBC	20.	HI
7.	BZP	21.	DI
8.	LD	22.	BOC
9.	LBP	23.	CIL
10.	BBP	24.	ZIL
11.	PPL	25.	ML
12.	LIF	26.	MH
13.	BIF	27.	IDL
14.	LM1_3	28.	IML

0.5 cm

FIG. 1.—Lateral, dorsal, and ventral views of skull and mandible showing the 28 craniomandibular measurements used in the morphometric analyses. Descriptions of the 28 variables are given in Supporting Information S1 (DOI: 10.1644/12-MAMM-A-276.S1).
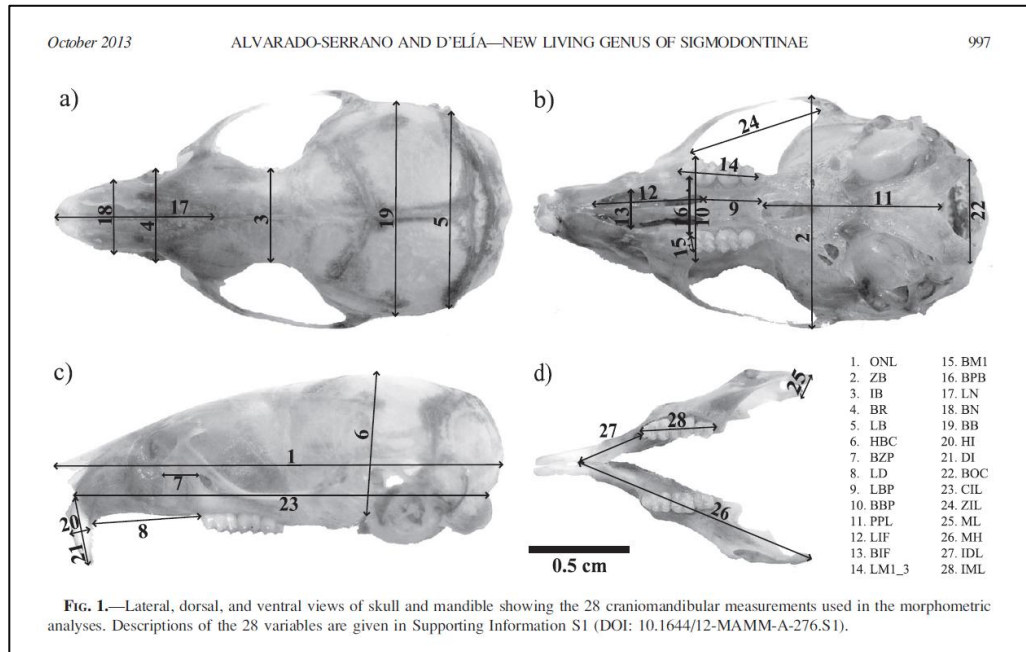
Figure 1. Measurements in this study, were based on various sources, including Alvarado-Serrano & D'Elía (2013).
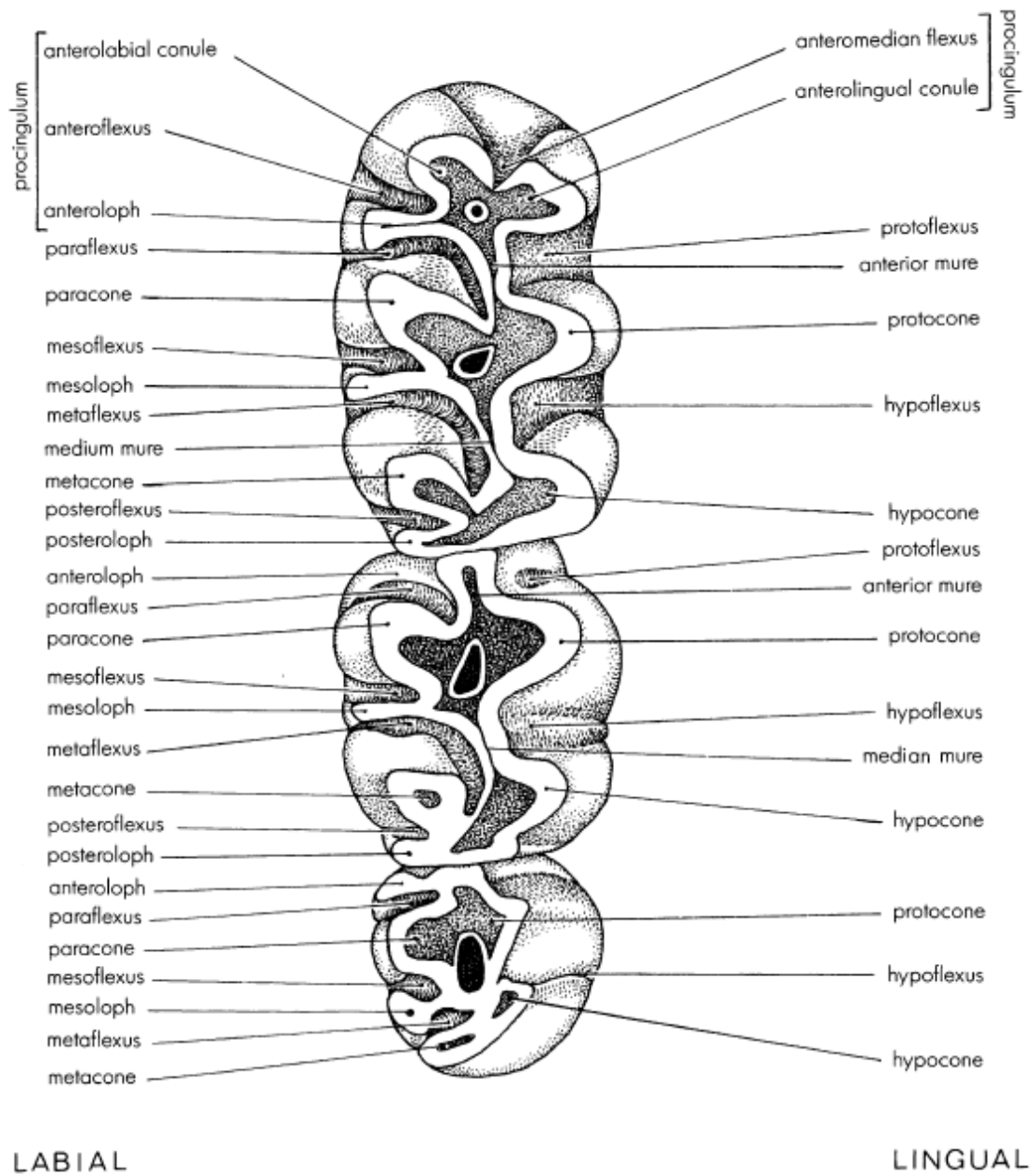
Figure 2. Dental characters and nomenclature analyzed in this study, from Carleton & Musser (1989).
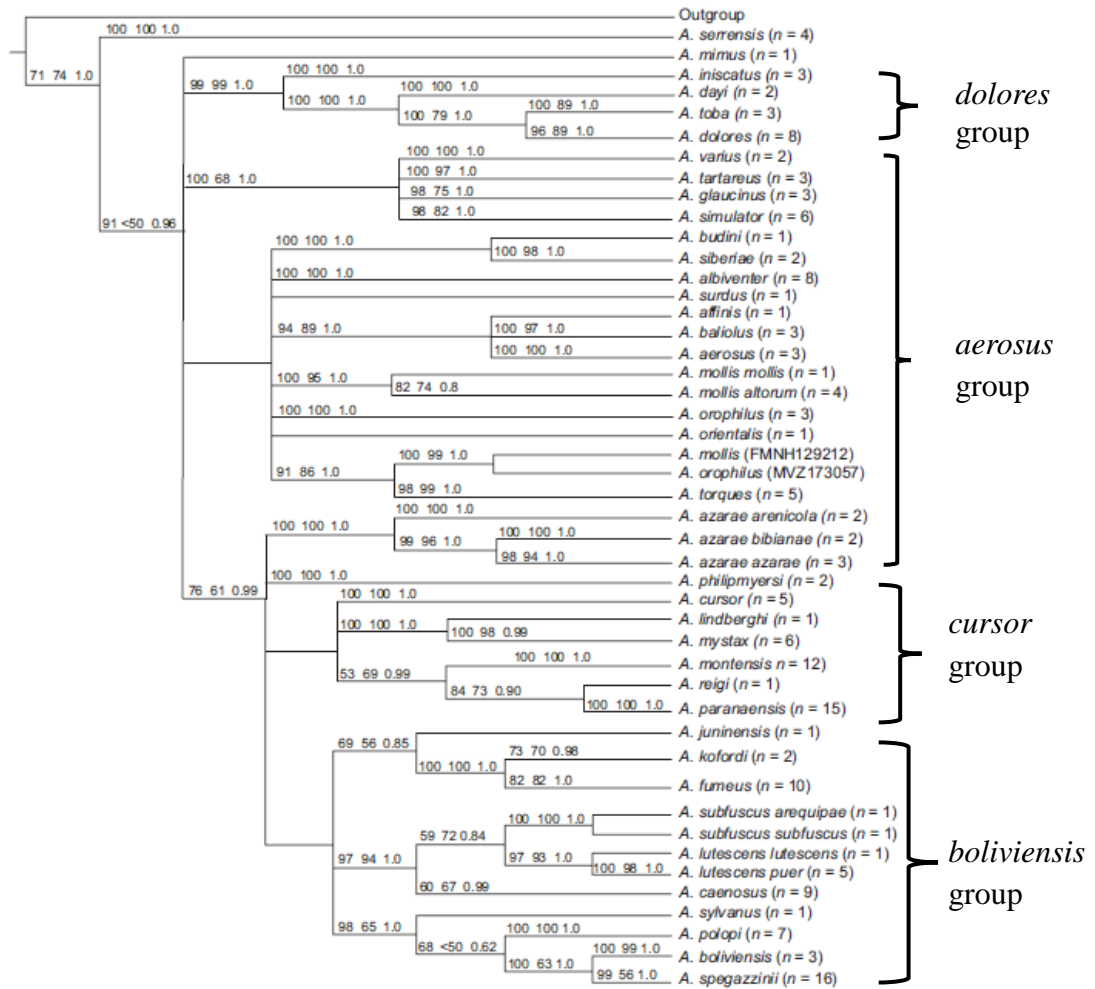
Figure 3. Phylogenetic tree of *Akodon* species and species groups, from Coyner et al. (2013). Species groups are circumscribed by brackets.
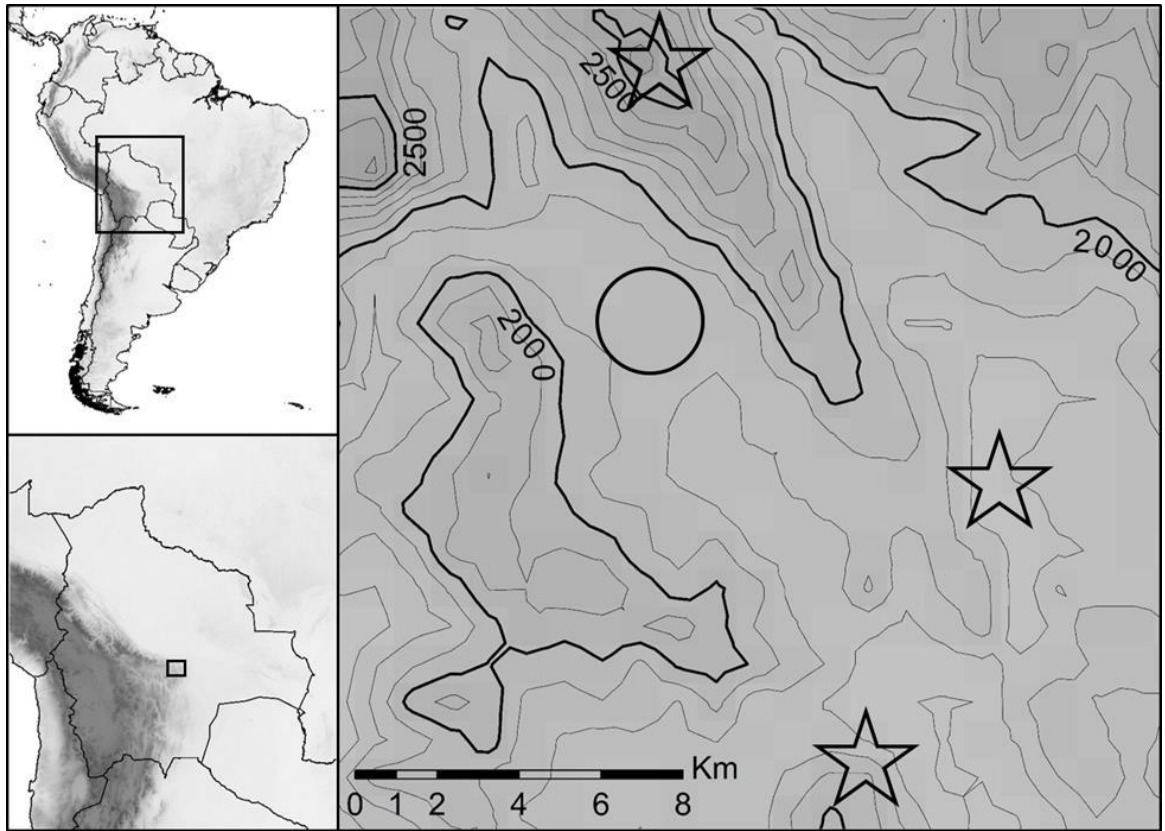
Figure 4. Trapping locations (represented by stars) around the town of Comarapa (represented by the circle). Elevational gradient is shown in grayscale. The Laguna Verde site is the northern most star. Upper left image shows Bolivia (inset) in South America; lower left image shows the study area in Bolivia.

Figure 5. A juvenile *Akodon siberiae* collected in Laguna Verde, near Comarapa.

Figure 6. Cladogram depicting the relationships among grass mice, genus *Akodon*, derived using sequences from the mitochondrial Cytochrome b gene. Individuals of *Akodon siberiae* collected in this study are indicated by a black circle. Brackets depict species groups. Asterisks indicate multiple species in a clade.
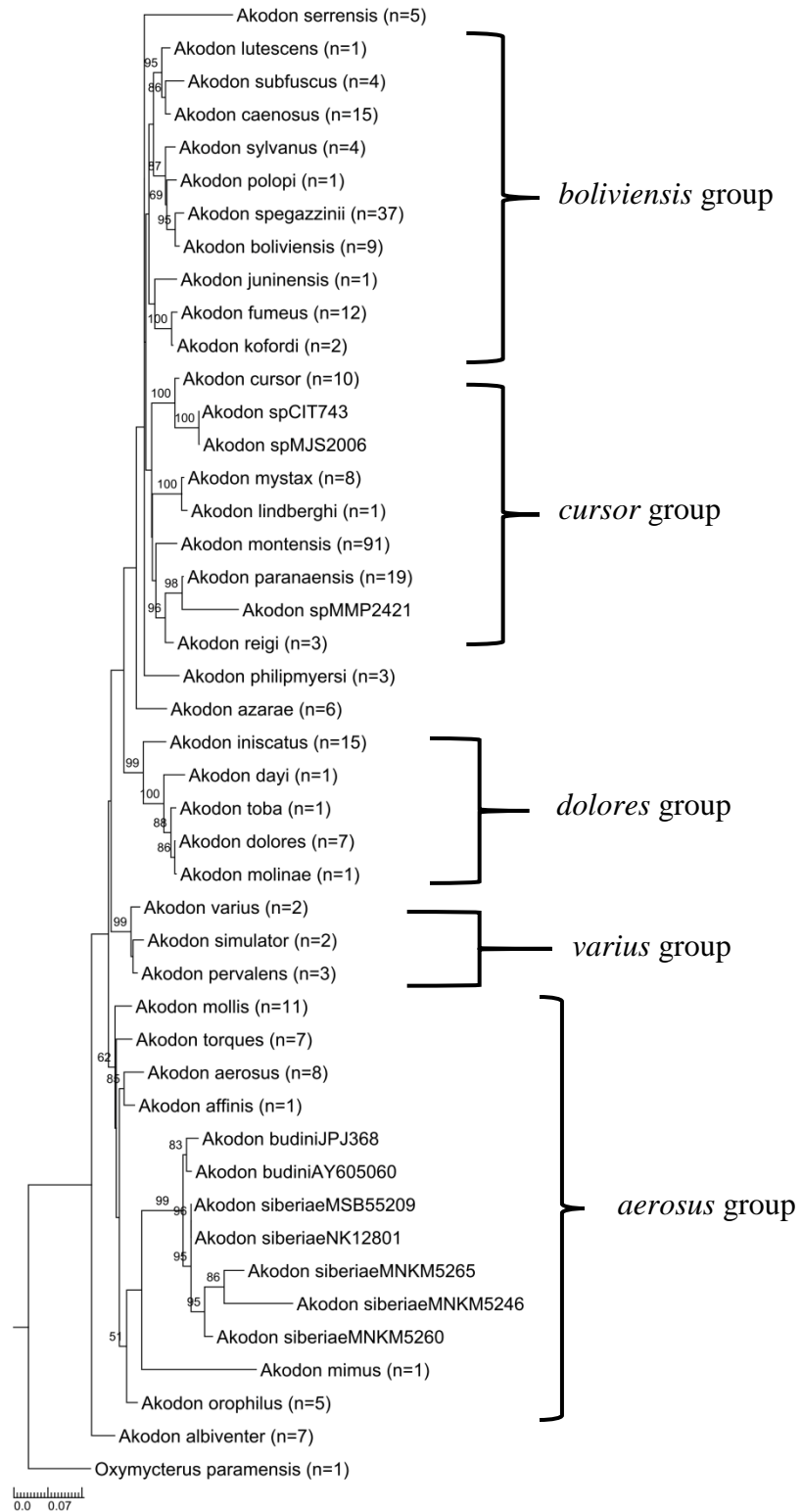
Figure 7. Phylogenetic tree derived using sequences cut to ≤801 bp. Bootstrap values above 50 percent shown.

Figure 8. Skull and mandible of *Akodon siberiae*, Museo Noel Kempff Mercado no. 5252, collected at the Laguna Verde site.
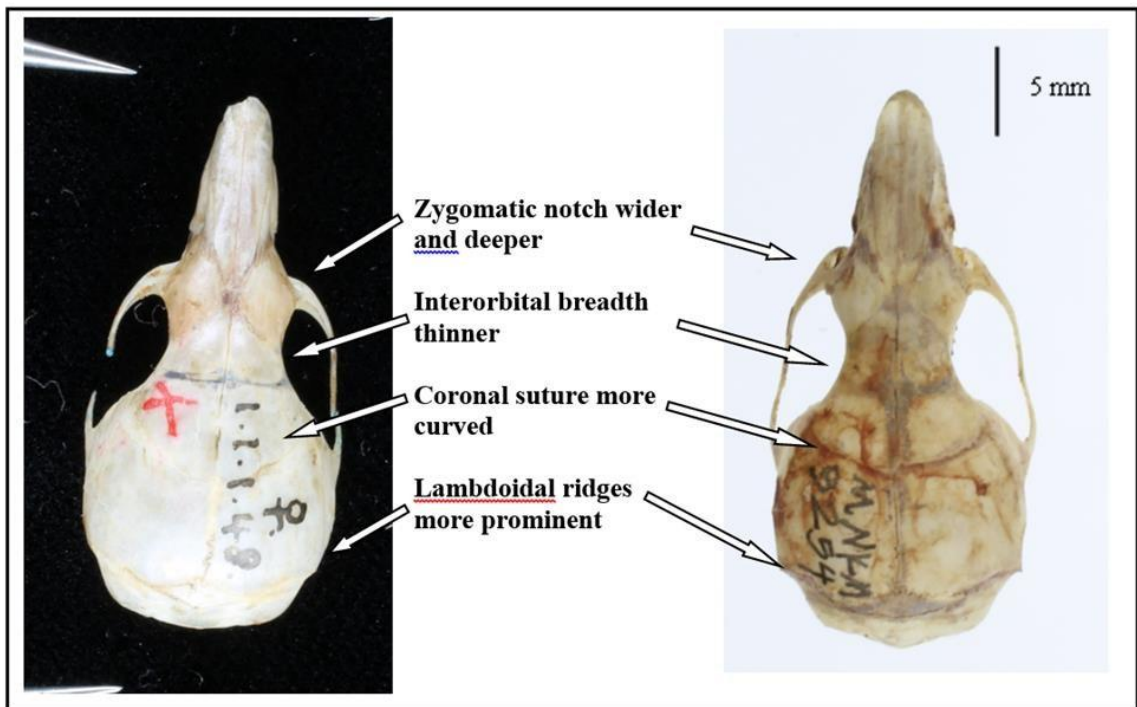
Figure 9. Dorsal view of the cranium of the holotype of *Akodon mimus* (MNH 1901.1.1.48) and *Akodon siberiae* specimen MNKM 5254, from Laguna Verde.
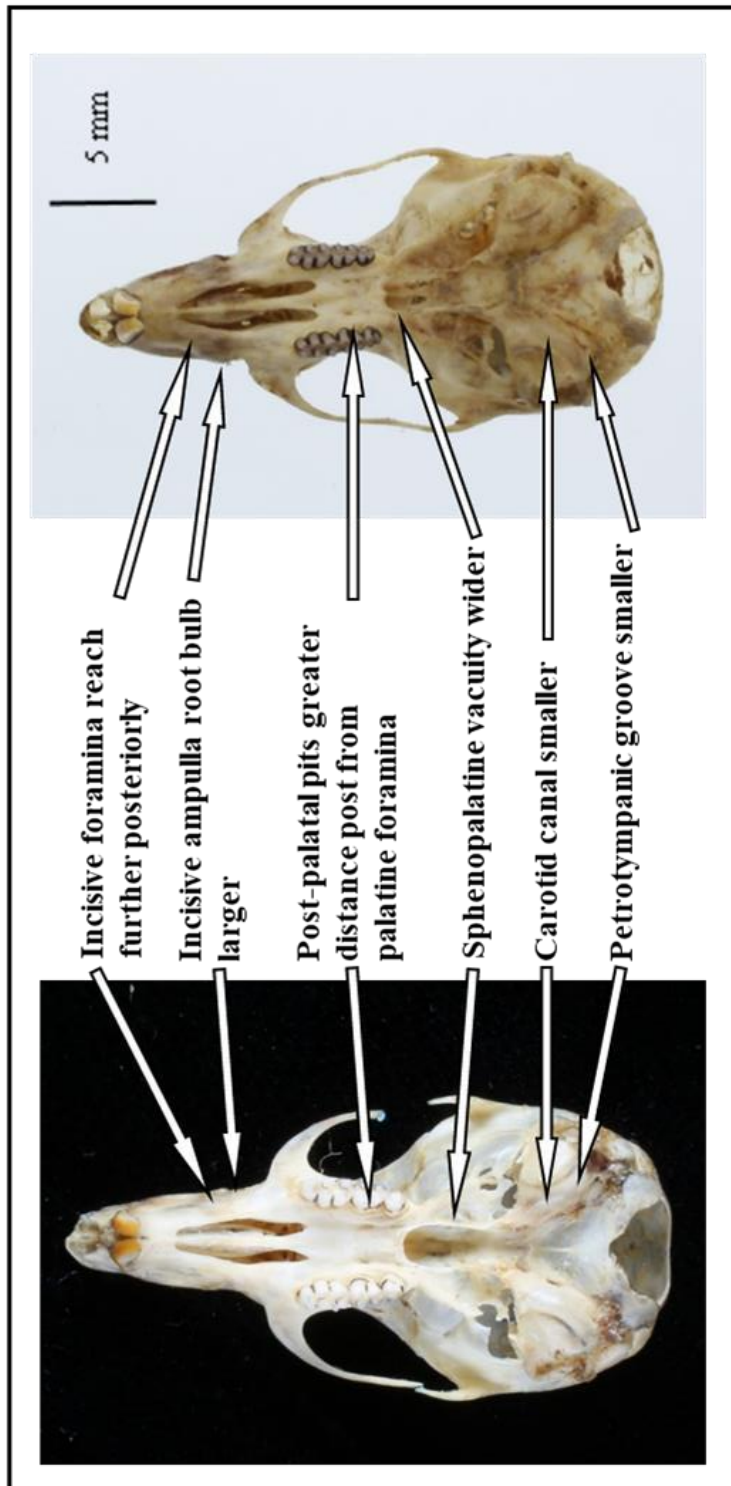
Figure 10. Ventral view of the cranium of holotype of *Akodon mimus* (MNH 1901.1.1.48) and a specimen *Akodon siberiae* from Laguna Verde (MNKM 5254). Critical similarities and differences are noted.
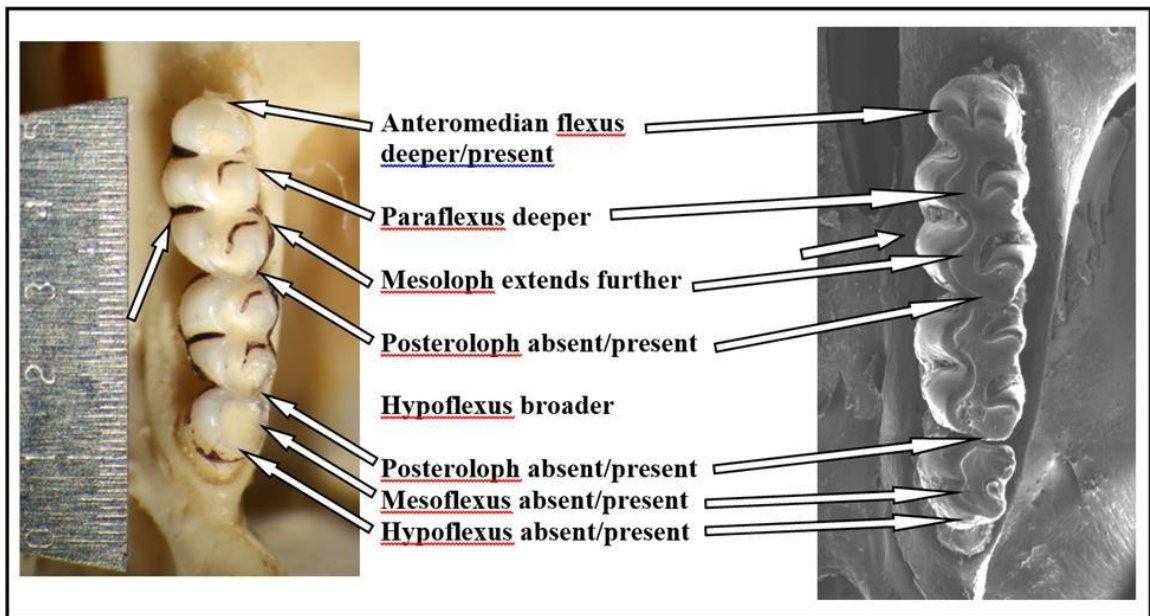
Figure 11. Comparison of dental features of the holotype of *A. mimus* (MNH 1901.1.1.48, left) and a scanning electron micrograph of a specimen of *A. siberiae* from Laguna Verde (MNKM 5254, right).

Figure 12. Lateral view of the skull of the holotype of *Akodon mimus* (MNH 1901.1.1.48). Note the caudally curved and thin zygomatic plate.
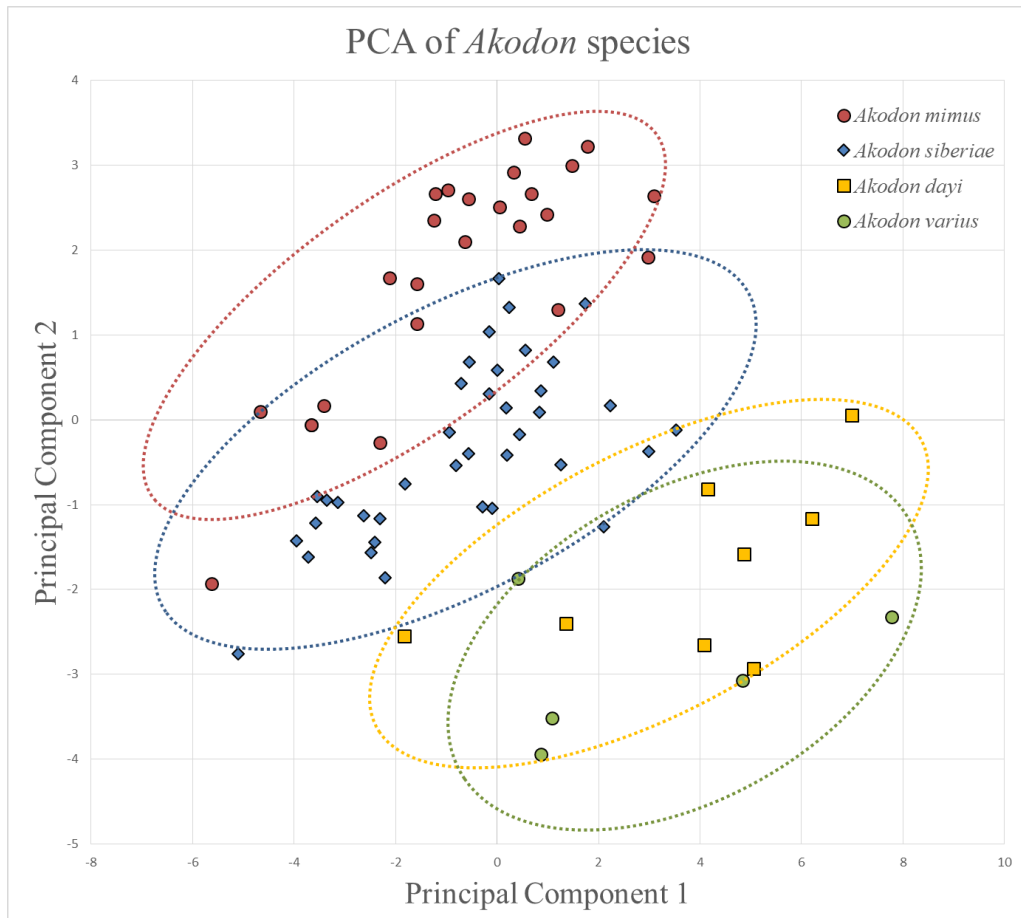
Figure 13. Graphical representation of the results of the principal component analysis carried out on 77 specimens of *Akodon dayi*, *A. mimus*, *A. siberiae*, and *A. siberiae* specimens from Comarapa.
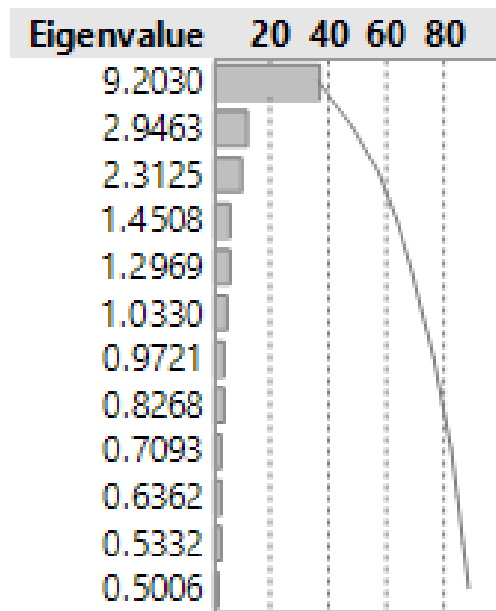
Figure 14. Eigenvalues resulting from the principal component analysis, with the percentage of explained variance for each (bar graph on right).
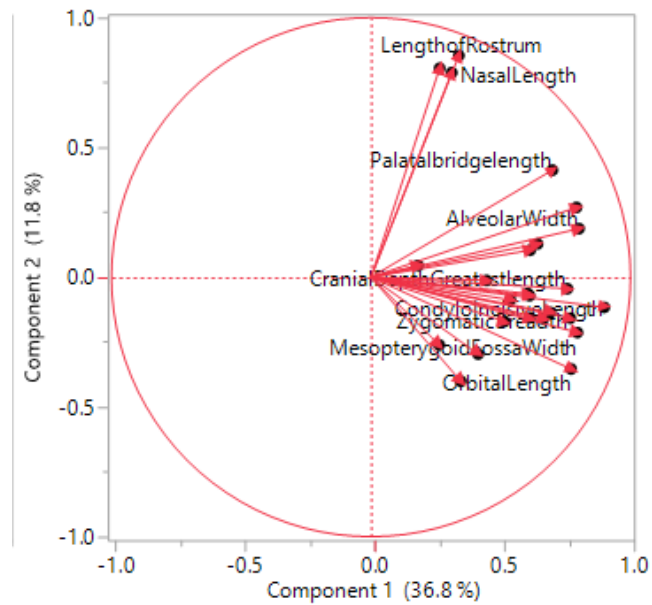
Figure 15. Loading plot, showing the variables used in the principal component analysis, and the relationship of each variable to PC1 and PC2.

45
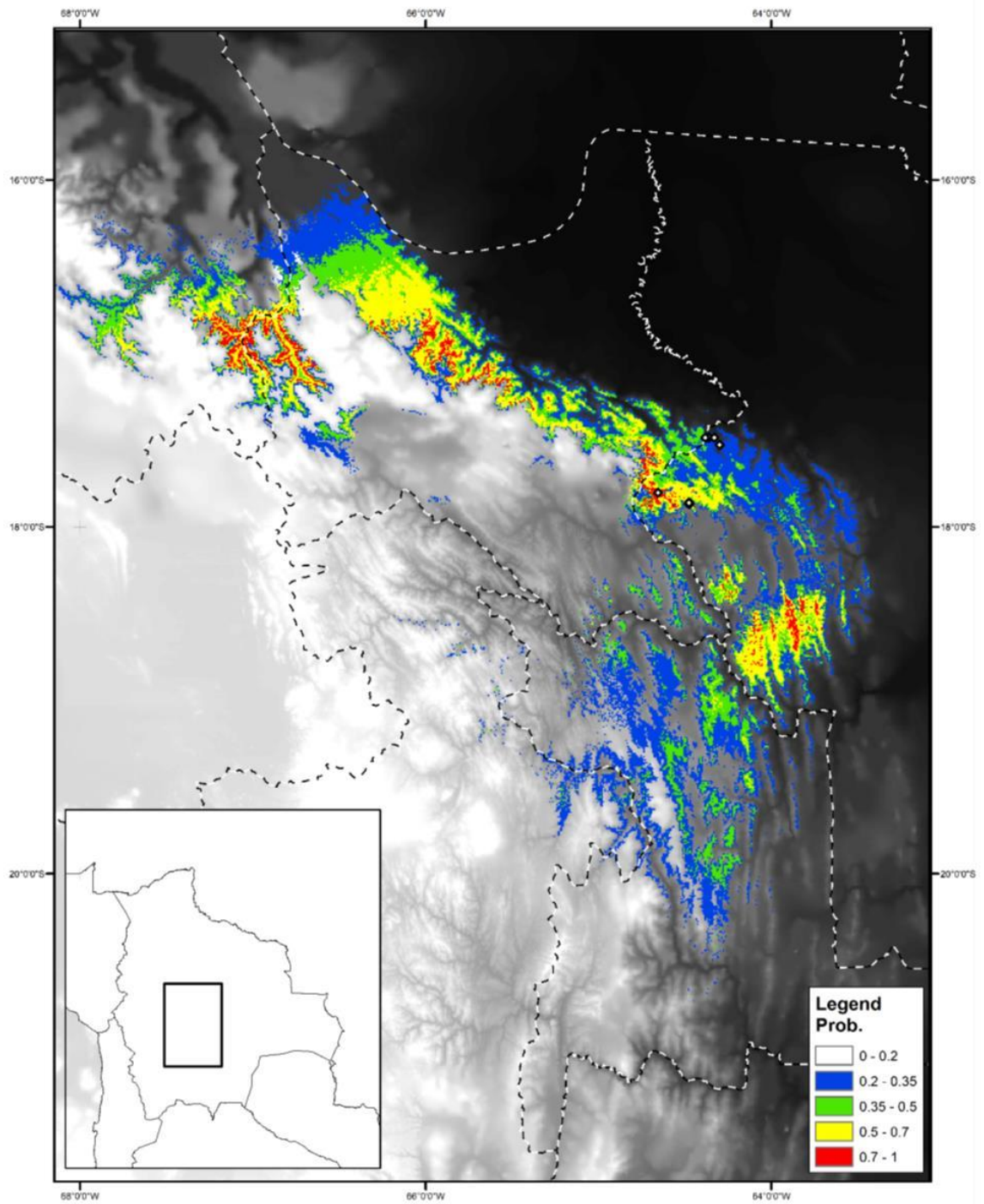
Figure 16. Environmental Niche Model depicting the probability of occurrence of *Akodon siberiae* in Bolivia, overlapped on the highest contributing bioclimatic variable: Elevation. Yellow dots indicate *A. siberiae* collecting sites, the furthest south being Comarapa.
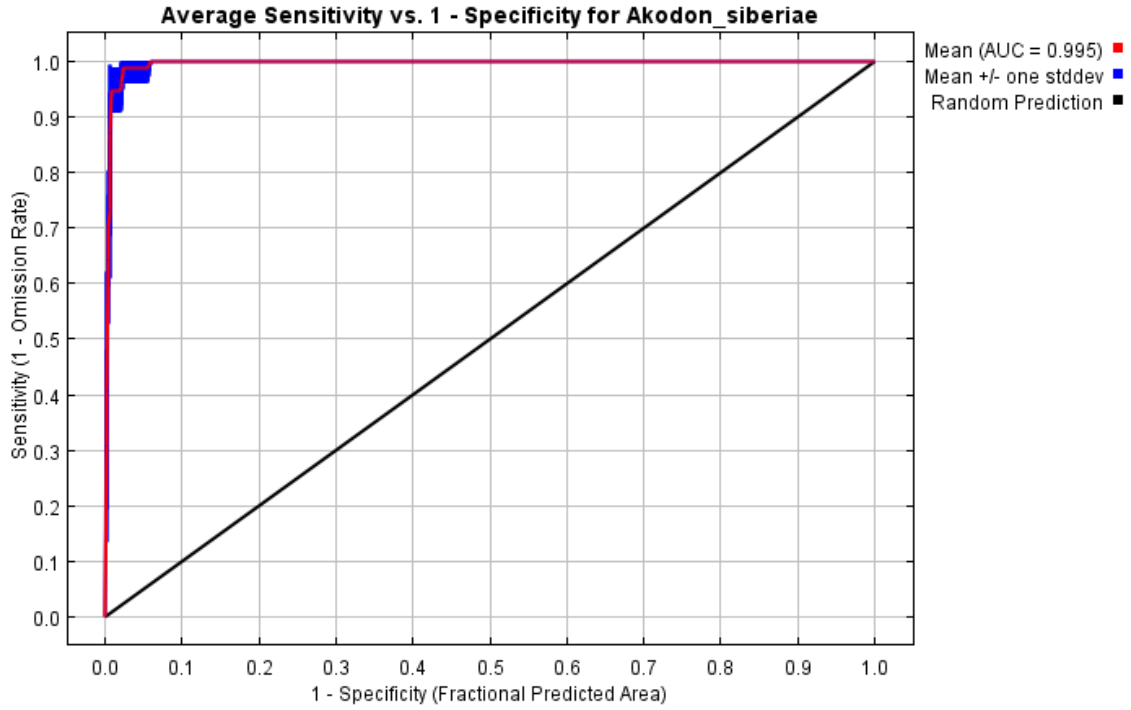
Figure 17. Graph of average sensitivity vs. 1-specificity for *Akodon siberiae*, with the mean area under curve and the standard deviation in blue. The black line represents a model that would have a random predictive power.
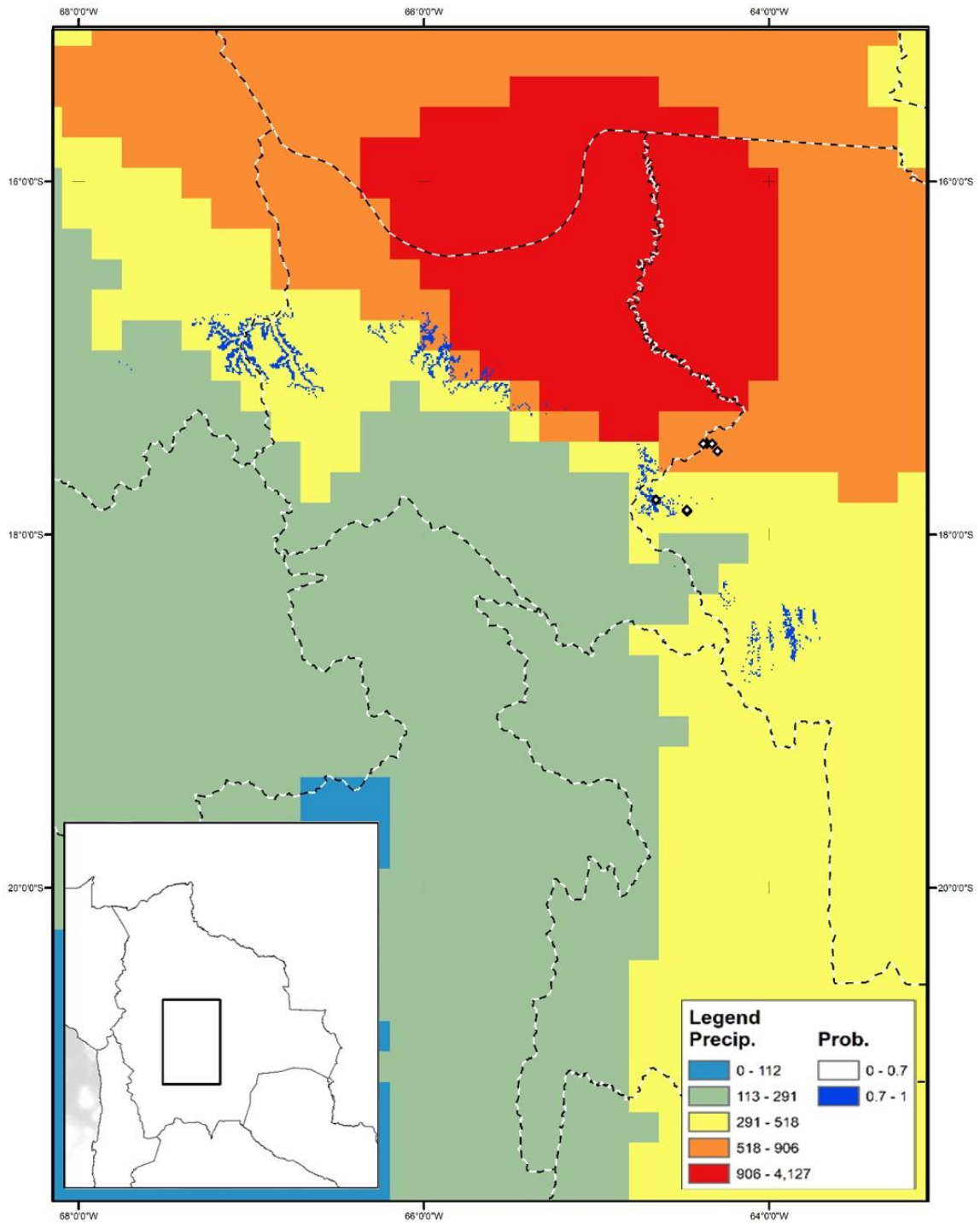
Figure 18. Environmental Niche Model depicting the probability of occurrence of *Akodon siberiae* in Bolivia, overlapped on the second highest bioclimatic variable: Precipitation during the warmest quarter.

References

Anderson, R. P., Peterson, A. T., & Gómez-Laverde, M. 2002. Using niche-based GIS modeling to test geographic predictions of competitive exclusion and competitive release in South American pocket mice. *OIKOS*. 98: 3–16.

Anderson, S. 1997. Mammals of Bolivia, taxonomy and distribution. *Bulletin of the American Museum of Natural History*. 231:1–652.

Alvarado-Serrano, D. F., D'Elía, G. 2013. A new genus for the Andean mice *Akodon latebricola* and *A. bogotensis* (Rodentia: Sigmodontinae). *Journal of Mammalogy*. 94(5):995-1015.

Bianconi, G., Mikich, S. B., & Pedro, W. 2006. Movement of bats (Mammalia, Chiroptera) in Atlantic Forest remnants in southern Brazil. *Revista Brasileira de Zoología.* 23(4): 1199–1206.

Bradley, R. D., & Baker, R. J. 2001. A test of the genetic species concept: cytochrome-b sequences and mammals. *Journal of Mammalogy,* 82(4): 960–973.

Burgin, C. J., Colella, J. P., Kahn, P. L., & Upham, N. S. 2018. How many species of mammals are there? *Journal of Mammalogy*. 99:1–11. [https://doi.org/10.1093/jmammal/gyx147]

Busby, J. R. 1986. A biogeoclimatic analysis of *Nothofagus cunninghamii* (Hook.) Oerst. in southeastern Australia. *Australian Journal of Ecology*. 11: 1–7.

Carleton, M. D., Musser, G. G. 1989. Systematic Studies of Oryzomyine rodents (Muridae, Sigmodontinae): A synopsis of *Microryzomys*. *Bulletin of the American Museum of Natural History*. 191:1–83.

Coyner, B. S., J. K. Braun, M. A. Mares, & R. A. van den Bussche. 2013. Taxonomic validity of species groups in the genus *Akodon* (Rodentia, Cricetidae). *Zoologica Scripta*. 42(4):335– 50. doi:10.1111/zsc.12014.

D'Elía, G. 2003. Phylogenetics of Sigmodontinae (Rodentia, Muroidea, Cricetidae), with special reference to the akodont group, and with additional comments on historical biogeography. *Cladistics*. 19: 307–323.

Evenstar, L. A., Stuart, F. M., Hartley, A. J., & Tattitch, B. 2015. Slow Cenozoic uplift of the western Andean Cordillera indicated by cosmogenic ^{3}He in alluvial boulders from the Pacific Planation Surface. *Geophysical Research Letters*. 42(20): 8448–8455.

Franklin, J., 1995. Predictive vegetation mapping: geographic modelling of biospatial patterns in relation to environmental gradients. *Progress in Physical Geography*. 19(4): 474–499.

Fridley, J. D., Senft, A. R., & Peet, R.K. 2009. Vegetation structure of field margins and adjacent forests in agricultural landscapes of the North Carolina Piedmont. *Castanea*. 74(4): 327–339.

Galbreath, E., Hafner, D. J., & Zamudio, K. R. 2009. When cold is better: climate-driven elevation shifts yield complex patterns of diversification and demography in an alpine specialist (American Pika, *Ochotona princeps*). *Evolution.* 63(11): 2848–2863.

Geise, L., M. F. Smith, and J. L. Patton. 2001. Diversification in the genus *Akodon* (Rodentia: Sigmodontinae) in Southeastern South America: Mitochondrial DNA sequence analysis. *Journal of Mammalogy*. 82(1): 92–101.

Ibisch, P. L., Rauer, G., Rudolph, D., & Barthlott, W. 1995. Floristic, biogeographical, and vegetational aspects of Precambrian rock outcrops (inselbergs) in Eastern Bolivia. *Flora*. 190: 299-314.

Janzen, D. H. 1967. Why mountain passes are higher in the tropics. *The American Naturalist*. 101(919): 233-249.

Jayat, J. P., Ortiz, P. E., Salazar-Bravo, J., Pardiñas, U. F. J., & D'Elía, G. 2010. The *Akodon boliviensis* species group (Rodentia: Cricetidae: Sigmodontinae) in Argentina: species limits and distribution, with the description of a new entity. *Zootaxa*, 2409: 1–61.

Kriticos, D. J., Webber, B.L., Leriche, A., Ota, N., Macadam, I., Bathols, J. & Scott, J.K. 2012. CliMond: global high resolution historical and future scenario climate surfaces for bioclimatic modelling. *Methods in Ecology and Evolution*. 3: 53–64. DOI: 10.1111/j.2041210X.2011.00134.x

Leite, R. N., Kolokotronis, S., Almeida, F. C., Werneck, F. P., Rogers, D. S., & Weksler, M. 2014. In the wake of invasion: Tracing the historical biogeography of the South American Cricetid Radiation (Rodentia, Sigmodontinae). *PLoS ONE*. 9(6): e100687.

López, R. P. & Zambrana-Torrelio, C. 2006. Representation of andean dry ecoregions in the protected areas of Bolivia: the situation in relation to the new phytogeographical findings. *Biodiversity and Conservation*. 15(7): 2163–2175. doi:10.1007/s10531-0046898-4.

Madriñan, S., Cortés, A. J., & Richardson, J. E. 2013. Páramo is the world's fastest evolving and coolest biodiversity hotspot. *Frontiers of Genetics*. 4:article 192. doi: 10.3389/fgene.2013.00192.

Martin, S. A., Alhajeri, B. H., & Steppan, S. J. 2016. Dietary adaptations in the teeth of murine rodents (Muridae): a test of biomechanical predictions. *Biological Journal of the Linnean Society*. 119: 766–784.

McCain, C. M. 2004. The mid-domain effect applied to elevational gradients: species richness of small mammals in Costa Rica. *Journal of Biogeography*. 31: 19–31.

Miller, M.A., Pfeiffer, W., & Schwartz, T. 2010 Creating the CIPRES Science Gateway for inference of large phylogenetic trees. *Proceedings of the Gateway Computing Environments Workshop (GCE)*, 14 Nov. 2010, New Orleans, Louisiana. 1–8.

Moraes R., M., Maldonado, C., & Zenteno-Ruiz, F. S. 2018. Endemic plant species of Bolivia and their relationships with vegetation. *IntechOpen*. doi:10.5772/intechopen.82776.

Myers, P., & Patton, J. 1989. A new species of *Akodon* from the cloud forests of Eastern Cochabamba department, Bolivia (Rodentia: Sigmodontinae). *Occasional Papers of the Museum of Zoology, The University of Michigan*. no. 720, 28 pp.

Myers, P., Patton, J., & Smith, M. F. 1990. A Review of the *Boliviensis* Group of *Akodon* (Muridae: Sigmodontinae), with Emphasis on Peru and Bolivia. *Miscellaneous Publications, Museum of Zoology, University of Michigan*. no. 177, 104 pp.

Nicholls, A. O. 1989. How to make biological surveys go further with generalized linear models. *Biological Conservation*. 50: 1–75.

Ockinger, E., Sweiger, O., Crist, T. O., Debinski, D. M., Krauss, J., Kuussaari, M., Peterson, J. D., Pöyry, J., Settele, J., Summerville, K. S., & Bommarco, R. 2010. Life-history traits predict species responses to habitat area and isolation: a cross-continental synthesis. *Ecology Letters*. 13: 969–979.

Olson, D. M., The distribution of leaf litter invertebrates along a Neotropical altitudinal gradient. *Journal of Tropical Ecology*. 10: 129–150.

Pardiñas, U. F. J., Teta, P., Alvarado-Serrano, D., Geise, L., Jayat, P. J. Ortiz, P. E., Goncalves, P. R., & D'Elía, G. 2015. Genus *Akodon*. Pp. 144-206 *in*: Mammals of South America Vol. 2. Edited by Patton, J. L., Pardiñas, U. F. J., & D'Elía, G. *The University of Chicago Press*.

Patterson, B. D., Stotz, D. F., Solari, S., Fitzpatrick, J. W., & Pacheco, V. 1998. Contrasting patterns of elevational zonation for birds and mammals in the Andes of southeastern Peru. *Journal of Biogeography*. 25(3):593–607.

Phillips, S. J., R. P. Anderson, and R. E. Schapire. 2006. Maximum entropy modeling of species geographic distributions. *Ecological Modelling*. 190: 231–259.

Plotzki, A., May, J. H., Preusser, F., & Veit, H. 2013. Geomorphological and sedimentary evidence for late Pleistocene to Holocene hydrological change along the Río Mamoré, Bolivian Amazon. *Journal of South American Earth Sciences*. 47: 230–242.

Reig, O. A., 1987. An assessment of the systematics and evolution of the Akodontini with the description of new fossil species of *Akodon* (Cricetidae: Sigmodontinae). *Fieldiana: Zoology*. 39: 347–399.

Roach, N. & Naylor, L. 2018. *Akodon siberiae*. The IUCN Red List of Threatened Species 2018: e.T757A22381246. http://dx.doi.org/10.2305/IUCN.UK.2018-1.RLTS.T757A22381246.en.

Ruedas, L. A. & Morales, J. C. 2005. Evolutionary relationships among genera of Phalangeridae (Metatheria: Diprotodontia) inferred from mitochondrial DNA. *Journal of Mammalogy*. 86(2):353–365.

Sergio, F. & Pedrini, P. 2007. Biodiversity gradients in the Alps: the overriding importance of elevation. *Biodiversity and Conservation*. 16(12): 3243–3254. doi:10.1007/s10531-0069113-y.

Sikes, R. S., and the Animal Care and Use Committee of the American Society of Mammalogists. 2016. 2016 Guidelines of the American Society of Mammalogists for the use of wild mammals in research and education. *Journal of Mammalogy*. 97(3): 663–688. DOI:10.1093/jmammal/gyw078

Sillero, N, 2011. What does ecological modelling model? A proposed classification of ecological niche models based on their underlying methods. *Ecological Modelling*. 222: 1343-1346. http://dx.doi.org/10.1016/j.ecolmodel.2011.01.018

Smith, M. F., & Patton, J. L. 1991. Variation in mitochondrial cytochrome b sequence in natural populations of South American Akodontine rodents (Muridae: Sigmodontinae). *Molecular Biology and Evolution*. 8(1): 85–103.

Smith, M. F., & Patton, J. L. 1993. The diversification of South American murid rodents: evidence from mitochondrial DNA sequence data for the akodontine tribe. *Biological Journal of the Linnean Society, London*. 50: 149–177.

Smithe, F. B. 1975. Naturalist's Color Guide. *The American Museum of Natural History*.

Stamatakis, A. 2014. RAxML version 8: a tool for phylogenetic analysis and post-analysis of large phylogenies. *Bioinformatics*. 30(9):1312–1313. https://doi.org/10.1093/bioinformatics/btu033

Thomas, O. 1918. On small mammals from Salta and Jujuy. *Annals and Magazine of Natural History*. 9(1):186-193.

Upham, N. S., Esselstyn, & J. A., Jetz, W. Ecological causes of uneven diversification and richness in the mammal tree of life. bioArxiv preprint:504803. Under consideration at *Proceedings of the National Academy of Sciences of the United States of America*.

Voss, R. S., Emmons, L. H. 1996. Mammalian Diversity in Neotropical lowland rainforests: A preliminary assessment. *Bulletin of the American Museum of Natural History*. 230:3–115.

Young, N., Carter, L., & Evangelista, P. 2011. A MaxEnt Model v.3.3.3e Tutorial (ArcGIS v10). Natural Resource Ecology Laboratory, Colorado State University.

Appendix I. Specimens examined

Species (n specimens used in morphological or genetic studies): **COUNTRY**: DEPARTMENT/PROVINCE: Locality: specimens found in locality by museum and collector numbers/Genbank Cyt b Accession#, sex M or F.

Akodon aerosus (6 specimens): **PERU**: CUSCO: 72 km NE by road Paucartambo, km 152: MVZ 171679/GenBank M35703, F. JUNIN: 10 km WSW by road of San Ramon, MVZ 172870 /GenBank M35707, F; MVZ 172871/GenBank M35708 M. PUNO: 4 km NNE of Ollachea: MVZ 172818/GenBankM35704) M; 14 km W of Yanahuaya: MVZ 172850/GenBank M35706, M; MVZ 172849/GenBank M35705, F.

Akodon aerosus baliolus (2 specimens): **BOLIVIA**: COCHABAMBA: 4.4 km N of Tablas Monte: MSB 70449/ GenBank KC841368, 400m. LA PAZ: Serrania Bella Vista, 1525 m, 15°41'S, 67°30'W MSB 68549/GenBank KC841366, F.

Akodon affinis (1 specimen): **COLOMBIA**: RISARALDA: Municipio Pereira, Corregimiento La Florida, vereda La Pastora, road to Las Cascadas, PRN Ucamarí, ICN 16547/GenBank AY196164).

Akodon albiventer (7 specimens): **ARGENTINA**: CATAMARCA: Paclin: 3.4 km S on Ruta Provincial 18, 1529 m, OMNH 30013/OCGR 4052/Arg 4802/GenBank KC841384. JUJUY: Yavi: 6.8 km SE of Suripujio, on Ruta Provincial No. 5, 3991 m, OMNH 30017/OCGR 3663/Arg 4732/GenBank KC841385. **CHILE**: TARAPACA: Colchane: Suricayo, 12 km N Enquelga, MSB 209890/NK 96060/GenBank AY341042; MSB 210396/NK 96068/GenBank AY341040. PARINACOTA: Parinacota: MSB 209869/NK96027/GenBank AY341041, F. Lago Chungara:MSB 209877/NK96043 /GenBank AY341039, M. Socoroma: MSB 209852/NK 96000/GenBank AY341037, M.

Akodon azarae (6 specimens): **ARGENTINA**: BUENOS AIRES: Punta Indio: CNP 751/GenBankAY702963. No locality information: As8/GenBank KJ9336944. **PARAGUAY**: ÑEEMBUCU: 5.8 km by road NE of Pilar: UMMZ 134443/GenBank U03529. PARAGUI: Coast of Tebicuary River: GD 264/GenBank DQ444328.1. **URUGUAY**: SAN JOSÉ: Kiyu: GD 327/GenBank AY702964. No locality information: GenBank EF622507.

Akodon boliviensis (9 specimens): **ARGENTINA**: Salta: 1 km ENE of Rodeo Pampa, km 59 of
Ruta Provincial N7, 3080 m: MACN 23507/ JPJ 1330/GenBank GU189321. Abra de Ciénaga Negra, 3 km SE, 3090 m: MACN 23499/GenBank GU189317; MACN 23500/GenBank GU189318. Azul Cuesta, aprox. 9 km S of Nazareno, 3286 m: MACN 23503/GenBank GU189319. Pampa Verde, aprox. 8 km WSW of Los Toldos and S of Cerro Bravo, 2400 m: MACN 23504/GenBank GU189320. **BOLIVIA**: TARIJA: 4.5 km E of Iscayachi, 21°29'S, 64°55'W, 3750 m: MSB 67141/NK 23619/GenBank KC841361; MSB 68571/NK 23620/GenBank KC841367. **PERU**: PUNO: 12 km S of

Santa Rosa (de Ayaviri) 3,950 m: MVZ 171607/GenBank M35691; MVZ 171608/GenBank M35692.

Akodon budini (2 specimens): **ARGENTINA**: Pampa Verde, 8 km WSW of Los Toldos and S of Cerro Bravo, 2,400 m: JPJ 368/GenBank EF166037. **BOLIVIA**: CHUQUISACA: Rinconada del Bufete, 20°49.81'S, 64°22.47'W, 2000 m: LHE 1260/GenBank AY605060.

Akodon caenosus (15 specimens): **ARGENTINA**: CATAMARCA: Ambato: El Rodeo: 1.5 km NE of Hwy 4, 1372 m: CML 3306/OCGR 1442/Arg 1545/GenBank KC841333; 6km SW of Hwy 9 on Hwy 18, 1524 m: OMNH 34355/OCGR 1330/Arg 1533/GenBank KC841387. Intersection of provincial highways N° 9 y 18, 3.4 km S, on Ruta Provincial N° 18, 1529 m: MACN23482/Genbank GU189322; MACN23483/Genbank GU189323. Bárcena, aprox. 3 km S, on Ruta Nacional N° 9, 1808 m: MACN 23494/GenBank GU189324. JUJUY: El Carmen: On highway 9 at border with Salta, at campground on the way to El Carmen, 1,402 m: OMNH 38619/OCGR 2136/Arg 2624/GenBank KC841406. San Antonio: Rio Blanco, 9 km SW San Antonio, 1495 m: OMNH 36486/OCGR 3500/Arg 4267/GenBank KC841391. SALTA: 1 km ENE of Rodeo Pampa, km 59 of Ruta Provincial N° 7, 3,080 m: MACN 23508/Genbank GU189326. Bárcena, aprox. 3 km S, on Ruta Nacional N° 9, 1808 m: MACN 23494/Genbank GU189324. Chicoana: 5 km WSW Pulares, 1482 m: OMNH 38640/OCGR 3707/Arg 4968/GenBank KC841407. Pampa Verde, aprox. 8 km WSW of Los Toldos and S of Cerro Bravo, 2400 m: MACN 23506/Genbank GU189325. TUCUMAN: aprox. 7 km NW of Usandivara property, Altos de Medina, 1717 m: MACN 23510/GenBank GU189327. **BOLIVIA**: CHUQUISACA: 2 km SW Monteagudo, 19.833°S, 64.983°W: MSB 63579/MSB NK 21380/GenBank KC841356. TARIJA: Abra Condor, ca 2 km W Junacas, 21.45°S, 64.4583°W, 2650 m: FMNH 162756/GenBank KC841344. Erquis, 21°28'S, 64°48'W, 2100 m: MSB 67134/MSB NK 23478/GenBank KC841359; km E of Tucumilla, 21°27'S, 64°49'W, 2500 m: MSB 67144/MSB NK 23670/GenBank KC841362.

Akodon cursor (10 specimens): **BRAZIL**: BAHIA: Estação Experimental Djalma Bahia, CEPLAC, Una, 15°18'S, 39°06'W, 28 m: EDH 30/GenBank AF184053. PARAÍBA: João Pessoa, 7°06'S, 34°51'W: GenBank EF206814. SÃO PAULO: Estação Biológica de Boracéia, Salesópolis, 22°11'S, 48°46'W, 850 m: MZUSP 29257/GenBank AF184051. Ilha do Cardoso: FMNH 141604/GenBank AF184052. 25.13°S, 47.97°W, 109 m: FMNH 141724/GenBank KC841340; FMNH 141622/GenBank KC841339. Fazenda Intervales, Capão Bonito: MVZ 182072/GenBank AF184049. Fazenda Capric6mrniUob, 23°024'S, 45°04'W, 150 m: MVZ 181075/Genbank AF184050. **PARAGUAY**: PARAGUARI: IBYCU I National Park, 32 km E (by road) from IBIC, 26.08° S, 56.8°W: MSB 67433/GenBank KC841363(RECORDED AS A. MONTENSIS ON TREE). No locality information: MN78918/GenBank KF815391.

Akodon dayi (15 specimens): **BOLIVIA**: SANTA CRUZ: Angel Sandoval: MNKM 580, MNKM 665, MNKM 666, MNKM 731, MNKM 799, MNKM 2665, MNKM 2682, MNKM 3723, MNKM 3743, MNKM 3757, MNKM 3724, MNKM 3725, MNKM 3905, MNKM 3908. PANDO: Remanso, 160 m (MSB NK 14376/GenBank EU260477).

Akodon dolores (7 specimens): **ARGENTINA**: CATAMARCA: Capayán: Chumbicha, 0.5 km E of Hwy 38 along Hwy 60, 457 m: OMNH 23527/OCGR 1516/Arg 1619/GenBank EU260473. MENDOZA: San Rafael: 2 km S Puesto Punta del Agua, 823 m: OMNH 36037/OCGR 10702/Arg 3113/CYTB GenBank KC841390. SAN LUIS: Capital: 15 km E Salinas del Bebedero, 411 m: OMNH 35926/OCGR 467/Arg 529/GenBank EU260472. Chacabuco: Papagallos: UP PY 16/GenBank AY273904. SANTIAGO DEL ESTERO: Atamisqui: 1 km northeast of junction Río Saladillo and highway 9, 213m: OMNH 35928/OCGR 1964/Arg 2353/GenBank EU260474. Guasayán: Virgen del Valle picnic area on highway 64 between Santa Catalina and La Puerta Chiquita, 701 m: OMNH 35929/OCGR 1917/Arg 2373/GenBank EU260476. Quebrachos: Buena Vista, 15 km NE Va. Ojo de Agua off of hwy 13, 396 m: OMNH 35927/OCGR 1964/Arg 2294/GenBank EU260475.

Akodon fumeus (12 specimens): **ARGENTINA**: JUJUY: Gral. Manuel Belgrano: 24.9 km N San Salvador, 1583 m: OMNH 38609/OCGR 7259/Arg 6662/GenBank KC841403. TUCUMÁN: Tafi: 12 km W of La Quebradita, Tafi del Valle, km 81 on Hwy 307, 2896 m:
OMNH 38608/OCGR 4012/Arg 4247/GenBank KC841402. SALTA: aprox. 5 km S of Los
Toldos, road to Vallecito, 1705 m: JPJ1656/GenBank GU189328; JPJ1670/GenBank GU189329. **BOLIVIA**: CHUQUISACA: Rinconada del Bufete, 20°49.81'S, 64°22.47'W, 2000 m: LHE 1262/CYTB GenBank AY605061. COCHABAMBA: Corani, 17°12'43"S,
65°52'4"W, 2630 m: MSB 70476/MSB NK 29793/GenBank KC841369. 21 KM (by road) W of Comarapa, 17.51°S, 64.27°W, 2900 m: AMNH 260580/MSB NK 12088/GenBank
KC841332. 28 km W (by road) Comarapa, 17°51'S, 64°40'W, 2800 m: MSB 55226/MSB NK 12020/GenBank KC841354. 4.4 km by rd N Tablas Monte, 17°04'S, 66°00'W, 1833 m: MSB 70703/MSB NK 30300/CYTB GenBank KC841371. Tinkusiri, 17 km E of Totora,
17°45'S, 65°02'W: MSB 87113/MSB NK 22858/GenBank KC841375. TARIJA: 5 km NNW Entre Rios, 21°29'S, 64°12'W, 1600 m: MSB 67139/MSB NK 23937GenBank KC841360. Pirulas, rd to Chiquiaca, 21.6532°S, 64.1025°W, 1550 m: FMNH 162755/GenBank KC841343.

Akodon iniscatus (15 specimens): **ARGENTINA**: NEUQUEN: Estáncia La Porteña, Sierra de Cuchillo Curá, Las Lajas: UP 442/GenBank AY605062. RIO NEGRO: Pilcaniyeu: 10 km S Comallo, 41.09°S, 70.21°W, 2900 m: MVZ 182655/GenBank AY273917. CHUBUT:
Puerto Lobos, 42° S, 65.07° W, 8 m: PNG1/GenBank HM167761. El Maitén, 42°06 S,

71.15°W: PNG1382bis/GenBank 167768. Gorro Figio, 43.04° S, 69.32°W, 352 m: PNG 1228/GenBank 167767. Campo de Pichiñan, 43.055° S, 69.06° W, 327 m: PNG 1204/GenBank HM167766. Piedra Grande, 43.72° S, 66.37° W, 70 m: PNG 1003/ GenBank 167762. Las Plumas, 43.72° S, 67.37° W, 167 m: PNG 1037/GenBank 167763. Cañadón Carbón, 43.84° S, 67.83° W, 203 m: PNG 1081/GenBank HM167764. Los Altares, 43.88° S, 67.27° W, 203 m: PNG 1170/GenBank HM167765. **CHILE**: AISEN: 1 km E Coyhaique Alto, 45.4833°S, 71.6°W, 730 m: FMNH 129845/GenBank KC841337; FMNH 129843/ Genbank HM167770, FMNH 129845/ GenBank HM167771.

Akodon juninensis (1 specimen): **PERU**: Junin, 22 km N of La Oroya, 4,040 m: MVZ 173038/GenBank M35698.

Akodon kofordi (2 specimens): **BOLIVIA**: LA PAZ: Rio Aceromarca, 16°19'S, 67°53'W, 2990 m: MSB 68528/MSB NK 25816/GenBank KC841365. **PERU**: PUNO: Agualani, 9 km N Limbani: MVZ 171665/CYTB GenBank M35697.

Akodon lindberghi (1 specimen): **BRAZIL**: MINAS GERAIS: MN 48026/GenBank AF184057.

Akodon lutescens lutescens (1 specimen): **PERU**: PUNO: 12 km S Santa Rosa (de Ayaviri): MVZ 171612/GenBank M35693.

Akodon mimus (47 specimens): **BOLIVIA**: COCHABAMBA: Coroni, 17°12'43" S, 65°52'09"
W, 2630 m: CBF 3496/NK 29849, M; CBF 3563/NK 29814, M; CBF3602/NK 29806, F; CBF 3616/NK 29802, M; CBF 3620/ NK 29780, M; CBF 3623/NK 29774, M; CBF 3624/NK 29820, M; CBF 3669 /NK 29781, M; CBF 3670/NK 29817, M; CBF 3677/NK 29803, F. Chapare, Hospital, Tranistional forest, Polylepis-Yunga, 3450 m: MHC 53/HOS
2, M; MHC 54/HOS 3, M; MHC 55/HOS 4, M; MHC 56/HOS 5, M; MHC 66/HOS 7, M; MHC 71/HOS 12, M. Tiraque, Comer C'ocha: Transitional forest, *Polylepis pepei*, near lagoon, 3882 m: MHC 6/SJ 6, F; MHC 7/SJ 7, F; MCH 8/SJ 8, M. Grassy/sparse *Polylepis* forest, 4290 m: MHC 4/SJ 4, M; MCH 5/SJ 5, F. MHC 10/SJ 10, M; MHC 13/SJ 13, F; MHC 58/SJ 14, F; MHC 59/SJ 15, M; MHC 60/SJ 16; MHC 61/SJ 16; MHC 63/SJ 19, M; MHC 65/SJ 21, M. LA PAZ: Franz tamayo, Palcabanba. 14°49'40" S 68°56'29" S, 2452 m:
MNKM 3598/NR 42, M; MNKM 3611/NR 55m M; MKNM 3599, M. 14°49'52" S 68°56'30" W, 2542 m: MNKM 3626 NR 70, M. Nor Yungas: Paramo del cerro Hornuni: 3550 m: CBF 7742/GVA 227, M; CBF 7755/GVA 200, F. PN-ANMF: CBF 7701/GVA 197, F. Mima Sueño, Cotapata, 2663 m: CBF 7684/GVA 94, F; CBF 7686/GVA 164. 2663 m: CBF 7686/GVA 164, M. Refuge of the 2nd climatic station, (Proyecto Yungas DFG-IE),

2534 m: CBF 7685/GVA 176; CBF 7742/GVA 227; CBF 7701/GVA 197. Pongo: FMNH 53984, M; FMNH 53985, M. **PERU**: Puno: 14 km W of Yanahuaya: MVZ 171712/ Genbank M35710, F; MVZ 171752/GenBank M35710.

Akodon molinae (1 specimen): No locality information: AK 222/GenBank AY494839.

Akodon mollis (6 specimens): **PERU**: ANCASH: Huari: Rio Mosna, between Chavin and San Marcos, 9.55° S, 77.17° W, 2926 m: FMNH129212/GenBank KC841334; QCAZ 4307/ GenBank HQ 731484; QCAZ 4998/GenBank HQ 731487; QCAZ 11271/GenBank HQ 731486; QCAZ 11285/GenBank HQ 731485.

Akodon mollis altorum (4 specimens): **ECUADOR**: AZUAY: "Cajas," 2°47'S, 79°13'W, 3870 m: MSB 196736/MSB NK 30901/GenBank KC841350; MSB 92704/MSB NK 30979/GenBank KC841376. BOLIVAR: Rio Tatahuazo, 2.5 km E of Cruz de Lizo, 1°43'S, 78°59'W, 2800 m: MSB 70722/MSB NK 27694/GenBank KC841372. CHIMBORAZO: Quebrada Guapo Chico, 1°58'S, 78°58'W, 2,000 m: MSB 70738/MSB NK 27725/GenBank KC841373.

Akodon mollis mollis (1 specimen): **PERU**: PIURA: "Machete" on Zapalache Carmen Trail: LSUMZ 27007/CYTB GenBank U03546.

Akodon montensis (91 specimens): **ARGENTINA**: CHACO, 7 km S Puerto Las Palmas, 27°10' S, 58°40' W: LTU594/GenBank JX538309; roe 281/GenBank KF207864; roe 282/GenBank KF207863. MISIONES: Puerto Iguazú, 25°35' S, 54°34' W: 34925/GenBank
JX538319. Wanda, 25°58' S, 54°33' W: 34865/GenBank JX538320. Parque Provincial Cruce Caballero, Carayá Pytá trail, 26°31' S, 53°59' W: LTU749/GenBank JX538310; LTU750/GenBank JX538311. Reserva Privada UNLP ''Valle del arroyo Cuña Pirú'', 27°05' S, 54°57' W: 15030003/GenBank JX538312; 15030005/GenBank JX538313; 15030006/GenBank JX538314; 15030014/GenBank JX538315; 16030003/GenBank JX538316; 16030004/GenBankl JX538317. Leandro N. Alem, 27°36' S, 55°19' W: 34766/
GenBank JX538318. **BRAZIL**: MATO GROSSO DO SUL, Facenda Maringá, 54 km W Dourados, 22°15'S, 55°17'W: MVZ197468/GenBank JX538321; MVZ197475/GenBank JX538322. MINAS GERAIS: Lagoa Santa, 19°38'S, 43°53'W: LS043II/GenBank AF184056. PARANÁ, Piraquara, Mananciais da Serra, 25°29'S, 48°58'W: LMT425/GenBank EF101873; LMT428/GenBank EF101874. RIO DE JANEIRO: Sumidouro, 22°12'S, 42°43'W: MCL28/GenBank JX538330. Nova Friburgo, 22°26'S, 42°32'W: LG48/GenBank JX538328; LG68/GenBank JX538329. Teresópolis, 22°23'S, 42°52'W: ML93/GenBank JX538331; EDH234/GenBank JX538332. Itatiaia, Brejo da Lapa, 22°23'S, 44°43'W: LG77/GenBank JX538327; MN48066/GenBank AY273906. SÃO PAULO: São José do Barreiro, 22°50'S, 44°41'W: EDH84/GenBank JX538338. Pedreiras, 22°43'S, 46°55'W: CRB1201/GenBank JX538335; CRB1204/GenBank JX538336. Río Claro, 22°24'S, 47°33'W: RTS6/GenBank JX538337. Araraquara, 21°47'S, 48°10'W: RTS22/GenBank JX538333. Boraceia, 22°11'S, 48°46'W:

FMNH141602/GenBank AF184055; MVZ192847/GenBank JX538334. Vicentinópolis, 20°55'S, 50°20'W: EDH61/GenBank JX538339. RIO GRANDE DO SUL, Rota do Sol, Tainhas–Terra de Areia, 29°26'S, 50°9'W: JR197/GenBank JX538323; JR198/GenBank JX538324; JR200/GenBank JX538325; JR203/GenBank JX538326. Tainhas, 29°16'S, 50°18'W: GenBank EF206813; GenBank EF206813. SANTA CATARINA, Jaborá, Linha

Safo, 27°10'S, 51°44'W: MN69917/GenBank EU251020; MN69920/GenBank EU251018; MN69925/GenBank EU251022; MN69933/GenBank EU251021. No locality information:

MN 78725/GenBank KF 815394; pm112/GenBank KJ 936956. **PARAGUAY**: CAAGUAZÚ, Estación San Ignacio, 24°59'S, 56°29'W: UMMZ133958/GenBank U03526.

CAAZAPÁ, Estancia Pytere, coast of Tebicuary River, 26°29.244'S, 55°53.825'W: UMMZ175057/GenBank JX538342; GD243/GenBank JX538347. 26°29.250'S, 55°53.907'W: GD222/GenBank JX538343; GD224/GenBank JX538344; UMMZ174866/GenBank JX538345; GD239/GenBank JX538346. ITAPÚA, Estancia Parabel, 26°29.352'S, 55°53.620'W: TK66181/GenBank JX538363; TK66182/GenBank JX538364; TK66183/GenBank JX538365; TK66184/GenBank JX538366. Estancia San Isidro, 5.18 km NW of houses, 26°29.284'S, 55°53.803'W: GD158/GenBank JX538367; UMMZ174849/GenBank JX538368; GD164/GenBank JX538369; GD176/GenBank JX538370; 4.91 km of houses, 26°29.352'S, 55°53.620'W: GD195/GenBank JX538371; GD214/GenBank JX538374; 5.56 km of houses, 26°29.095'S, 55°53.898'W: UMMZ175042/GenBank JX538372; GD209/GenBank JX538373. Estancia Golondrina, 25°33.54'S, 55°29.17'W: TK63626/GenBank JX538340; TK63629/GenBank JX538341. CANINDEYÚ, Reserva Natural Privada Itabó, 24°27.47'S, 54°39.85'W: TK63411/GenBank JX538356; TK63412/GenBank JX538357; TK63413/GenBank JX538358. Chupa Pou, 7.33 km from entry 24°09.905'S, 55°42.301'W: UMMZ175054/GenBank JX538348; 8.07 km NW of entry, 24°09.456'S, 55°42.366'W: GD131/GenBank JX538349; GD135/GenBank JX538351; GD136/GenBank JX538352; GD137/GenBank JX538353; 8.29 km of entry, 24°09.330'S, 55°42.386'W: GD134/GenBank JX538350. Reserva Natural del Bosque Mbaracayú, 24°08.75'S, 55°19'W: TK61794/GenBank JX538359: 8; TK64031/GenBank JX538362. 24°09.61'S, 55°16.99'W: TK63979/GenBank JX538360; TK64004/GenBank JX538361. Estancia Felicidad, 39 km NW of houses 24°09.411'S, 55°2,281'W: GD097/GenBank JX538354. 5.16 km WNW of houses 24°09.633'S, 55°42.261'W: UMMZ175048/GenBank JX538355. CORDILLERA, Emboscada, 25°6'S, 57°19'W: GD513/GenBank AY195864.

ÑEEMBUCÚ, Estancia San Felipe, 27°11.12'S, 58°23.27'W: TK66060/GenBank JX538375. Estancia Yacare´, 323 km of Puesto San Fernando, 26°33.991'S, 58°06.961'W:

UMMZ174827/GenBank JX538376. 26°38.42'S, 58°04.89'W: TK64349/GenBank JX538377. 26°39.07'S, 58°03.33'W: TK64387/GenBank JX538378. PARAGUARÍ, Parque

Nacional Ybycu'i, 26°04.64'S, 56°50.98'W: TK63781/GenBank JX538379;

TK63783/GenBank JX538380; TK63786/GenBank JX538381. Sapucai, Property of Mr. Americo Monges: UMMZ 174969/GenBank AY273905; MN69918/GenBank EU251023.
SAN PEDRO, Choré, Ganadera Jejui, 1.8 km SE of houses, 24°07.154'S, 56°25.280'W: UMMZ174891/GenBank JX538382.

Akodon mystax (8 specimens): **BRAZIL**: RIO DE JANERIO: Arrozal: MN 65565/GenBank EF101875; MN 69566/GenBank EF101876; MN 69567/GenBank EF101877; MN 69627/GenBank EF101878; MN 69629/GenBank EF101879; MN 69660/GenBank EF101880; MNJ35927/GenBank AF184054. No locality information: MN48070/GenBank AY277428.

Akodon orophilus (5 specimens): **PERU**: AMAZONAS: Chachapoyas: ca 20 km by road W Leimebamba, 6.75°S, 77.8°W, 2804 m: FMNH 129234/GenBank U03524; FMNH 129235/GenBank KC841335; FMNH 129237/GenBank KC841336. JUNIN: 16 km NNE Palca: MVZ 173057/GenBank M35699. HUANUCO: Unchog, pass between Churrubamba and Hda. Paty, NNW Acomayo, 3450 m: LSUMZ 27957/GenBank U03547.

Akodon parananses (16 Speciemsn) **BRAZIL**: MINAS GERAIS: Brejo da Lapa, Itatiaia, Itamonte: MN 48041/GenBank AF184054 (as *A. mystax*). RIO DE JANEIRO: Campos do Itatiaia, Abrigo Rebouças, Pq. Nac. Itatiaia: MN 69686/GenBank EF101886; MN 69700/GenBank EF101887; MN 69726/GenBank EF101888. RÍO GRANDE DO SUL: Parq. Nac. Aparados da Serra: LMT 270/GenBank EF101881; LMT 294/GenBank EF101882. Venancio Aires: CIT 1131/GenBank AY195866. SANTA CATARINA: Urubici: LMT 301/GenBank EF101883; LMT 304/GenBank EF101884. **PARAGUAY**: TTU TK 66311/GenBank EU579471. Locality information unknown: LMT 405/GenBank
EF101885; MN 48070/GenBank AY273907; MN 69930/GenBank EU251017; MN 69931/GenBank EU251019; GenBank EF622506. TK66278/GenBank EF621304; TK66185/GenBank EF621303; CIT1342/GenBank EF621302.

Akodon pervalens glaucinus (3 specimens): **ARGENTINA**: CATAMARCA: Andalgalá: Ambato: El Rodeo, 1.5 km NE of Hwy 4, 1372 m: OMNH 23699/OCGR 1441/Arg 1544/GenBank EU260483. Choya, 13 km NNW of Andalgalá, 1219 m: OMNH 23671/OCGR 1697/Arg 2038/GenBank EU260484. 3.4 km S intersection of highways 18 and 9, on Ruta Provincial No. 18, 1529 m: OMNH 30013/OCGR 4052/Arg 4802/GenBank KC841384.

Akodon philipmyersi (3 specimens): **ARGENTINA**: MISIONES: Posadas: Estancia Santa Inés, Ruta No. 105 km 10, 27°31'32"S, 55°52'19"W, 95 m: CNP 739/GenBank AY702965; CNP 741/GenBank AY702967; CNP 742/GenBank AY702966.

Akodon polopi (1 specimen): **ARGENTINA**: CÓRDOBA: Pampa de Achala, aprox. 6 km (on route 34) E of antenna La Posta, 2200 m: MACN 23486/GenBank GU189330.

Akodon reigi (3 specimens): **URUGUAY**: LAVALLEJA: Paso Averías: MNHN 3682/GenBank AY195865. GD 624/GenBank EF621305. No locality information: SBV2/GenBank KJ936959.

Akodon serrensis (5 specimens): **BRAZIL**: RIO DE JANEIRO: no exact locality: MN 35927/GenBank AF184058; Vale das Antas, Parque Nacional da Serra dos Órgãos: VA 1/GenBank AY273908. SANTA CATARINA: Urubici: LMT 436/GenBank EF101889. Locality information unknown: GenBank EF622508; pm102/GenBank KJ936954.

Akodon siberiae (66 specimens): **BOLIVIA**: SANTA CRUZ: Comarapa, Laguna Verde Park: MNKM 5238; MNKM 5239; MNKM 5240; MNKM 5241; MNKM 5242; MNKM 5243; MNKM 5244; MNKM 5245; MNKM 5246; MNKM 5247; MNKM 5248; MNKM 5249; MNKM 5250; MNKM 5251; MNKM 5252; MNKM 5253; MNKM 5254; MNKM 5256; MNKM 5259; MNKM 5260; MNKM 5261; MNKM 5262; MNKM 5264; MNKM 5265; MNKM 5266; MNKM 5267; MNKM 5268; MNKM 5269; MNKM 5270; MNKM 5271; MNKM 5272; MNKM 5273; MNKM 5274; MNKM 5275; MNKM 5276; MNKM 5277; MNKM 5278; MNKM 5279; MNKM 5280; MNKM 5281; MNKM 5282; MNKM 5283; MNKM 5284; MNKM 5285; MNKM 5286; MNKM 5287; MNKM 5288; MNKM 5289; MNKM 5290; MNKM 5294; MNKM 5296; MNKM 5297; MNKM 5298; MNKM 5299; MNKM 5287; MNKM 5252; MNKM 5253; MNKM 5254; MNKM 5288. COCHABAMBA: 28 km by road W of Comarapa, 17°55'S, 64°40'W, 2800m: MSB 55209/Genbank U03548, M. 31 km by road W of Comarapa, 2800m: MSB NK 12801/AMNH M 260578/MSB 210733/Genbank AY273909; FMNH 260423; FMNH 260426; FMNH 260427; FMNH 260428; FMNH 260430, M; FMNH 260578; FMNH 260579. 17°51'S, 64°40'W, 2800m: FMNH 260431, F.

Akodon simulator (6 specimens): **ARGENTINA**: JUJUY: San Antonio: Río Blanco, 9 km SW San Antonio, 1495 m: OMNH 33094/OCGR 3510/Arg 4288/GenBank EU260480; Santa
Barbara: 5 km E El Palmar, 794 m: OMNH 38617/OCGR 7462/Arg6906/GenBank KC841405. SALTA: Chicoana: 5 km WSW Pulares, 1482 m: OMNH 30014/OCGR 3708/Arg 4969/GenBank EU260482; OMNH 38647/OCGR 3710/Arg 4971/GenBank KC841408; Rosario de la Frontera: Finca Barba Yaco, 8.5 km SE Ojo de Agua, 1347 m: OMNH 29994/OCGR 3643/Arg 4678GenBank KC841383. TUCUMÁN: Monteros: Reserva La Florida, 7 km W Ibatín, Río Pueblo Viejo, 515 m: OMNH 30004/OCGR 3449/Arg 4074/GenBank EU260481.

Akodon spegazzinii (37 specimens): **ARGENTINA**: CATAMARCA: Andalgala: Choya, 13 km NNW of Andalgala, 1,219 m: OMNH 23458/OCGR 1678/Arg 2011/GenBank KC841380.
Santa Maria: 21 km SW El Desmonte, 2172 m: OMNH 37288/OCGR 9646/Arg 4502/GenBank KC841393. Planta Caimancito, well 43, 560 m: JPJ 2048/GenBank

GU189348. El Bolsón, 2309 m: JPJ 2076/GenBank GU189347; JPJ 2084/GenBank GU189348; JPJ 2085/GenBank GU189346. Mogote Las Trampas, aprox. 15 km al NW de
Chumbicha, 2300 m: JPJ 1476/GenBank GU189345; MACN 23479/GenBank GU189335.
Mogote Las Trampas, aprox. 15 km NW, Chumbicha, 2300 m: MACN 23479/GenBank GU189335; MACN 23480/GenBank GU189336. km 33 de la Ruta Provincial Nº 47, S of Capillitas, 2500 m: MACN 23476/GenBank GU189332. Laguna Blanca, 3243 m: MACN 23477/GenBank GU189333; MACN 23478/GenBank GU189334. MENDOZA: Lujan de Cuyo: approx. 3 km SSE Vallecitos (by road) 2193 m: OMNH 37496/Arg 4011/GenBank KC841397; OMNH 37498/Arg 4021/GenBank KC841398. Cachi Adentro, Río Cachi, 2490 m: MACN 23495/GenBank GU189337. SALTA: Cachi: approx. 3 km N Cachi Adentro,
2724 m: OMNH 36501/OCGR 4104/Arg 4992/GenBank KC841392; CML uncatalogued/OCGR 4105/Arg 4994/GenBank KC841379; Chicoana: app. 15 km al W de
Escoipe, Ruta Prov. No. 33, 2680 m: OMNH 33006/OCGR 4059/Arg 4818/GenBank KC841386. Aprox. 15 km W of Escoipe, on Ruta Provincial Nº 33, 2680 m: MACN 23496/GenBank GU189338; MACN 23497/GenBank GU189339. SAN JUAN: Iglesia: Tudcum, "Nacedero", 2,030 m: OMNH 37505/OCGR 349/Arg 401/GenBank KC841399;
OMNH 37506/OCGR 350/Arg 402/GenBank KC841400. TUCUMÁN: Burruyacu: Piedra
Tendida, 12 km WNW Burruyacu along Rio Cajon, 760 m: OMNH 37375/OCGR 952/Arg
1052/GenBank KC841394; Monteros: Reserva La Florida, 7 km W Ibatín, Río Pueblo Viejo, 515 m: OCGR 3469/Arg 4160/GenBank KC841378; Tafi: El Infiernillo, km 83 along Rt 307, 3048 m: OMNH 23647/OCGR 1222/Arg 1324/GenBank KC841381; Tafi del Valle: 2 km below La Heradera along Hwy 307, 1,067 m: OMNH 37398/OCGR 1307/Arg
1410/GenBank KC841395; Tafi del Valle: La Quebradita, km 69 along Hwy 307, 2,286 m:
OMNH 23654/OCGR 1328/Arg 1431/GenBank KC841382; Trancas: km SW de Hualinchay, 2822 m: OMNH 38584/OCGR 3691/Arg 4880/GenBank KC841401; Yerba Buena: 4 km west of junction hwy 338 and road to Horco Molle, along hwy 338 (road to San Javier), 838 m: OMNH 37431/OCGR 1807/Arg 2179/GenBank KC841396. Carapunco, km 81 de la Ruta Provincial N° 307, 2960 m: CNP 1491/GenBank GU189344. Parque
Biológico Sierra de San Javier, university residential area, LIEY, 711 m: MACN 23515/GenBank GU189342. La Cruz, Cumbre del Taficillo, Parque Biológico Sierra de San Javier, 1907 m: MACN 23512/GenBank GU189341; CNP 1490/GenBank GU189343. No locality information: JPJ 1190/GenBank DQ683182; OGCR 3469/GenBank KC841378; OGCR 4105/GenBank KC841379.

Akodon subfuscus (2 specimens): **PERU**: CUSCO, 26 km NW Ollantaytambo, 3,700 m: MVZ 174229/GenBank M35696; PUNO: 6.5 km SW Ollachea, 3,350 m: MVZ 172969/GenBank M35694.

Akodon subfuscus arequipae (1 specimen): **PERU**: AREQUIPA: 15 km S Callalli: MVZ 174109/GenBank M35695.

Akodon subfuscus subfuscus (1 specimen): **PERU**: APURIMAC: 36 km S (by road) Chalhuanca,
16.55°S, 73.31°W, 3510 m: MVZ 174239/GenBank KC841377.
Akodon sylvanus (4 specimens): **ARGENTINA**: JUJUY: Santa Barbara: 24.8 km E Santa Clara, 1,321 m: OMNH 38610/OCGR 7417/Arg 6861/GenBank KC841404. Finca El Piquete,
Volcán, aprox. 5 km from Río Tamango and logging road, 973 m: MACN 23490/GenBank GU189349. La Herradura, 12 km SW El Fuerte, on Ruta Provincial N° 6, 1428 m: JPJ 590/GenBank DQ683180. No locality information: JPJ 925/GenBank DQ683181.

Akodon tartareus (2 specimens): **BOLIVIA**: TARIJA: 3 km SE of Cuyambuyo, 22°16'S, 64°33'W, 900 m: AMNH 264333/MSB NK 23741/GenBank EU260486. 5 km W of Estancia Bolivar, 21°38'S, 62°34'W, 400 m: MSB 67183/MSB NK 23980/GenBank EU260487.

Akodon toba (4 specimens): **ARGENTINA**: CHACO: Pampa del Indio: roe 330/GenBank KF207858. **PARAGUAY**: BOQUERON: Filadelfia Martens, 22°20'40"S, 60°01'54"W, 100 m: MSB 80493/MSB NK 72371/GenBank KC841374. PRESIDENTE HAYES: 8 km NE Juan de Zalazar: UMMZ 133965/GenBank U03527. No exact locality: TTU TK 66486/CYTB GenBank AY273910 as A. varius).

Akodon torques (7 specimens): **PERU**: CUSCO: La Esperanza, 13°10.664'S, 71°36.271'W, 2880 m: FMNH 174966/GenBank KC841347; FMNH 175011/GenBank KC841348; FMNH 175033/GenBank KC841349. 32 km NE Paucartambo: MVZ 171720/GenBank M35700; MVZ 171721/GenBank M35701. Pillahuata, 13.16219°S, 71.59750°W: FMNH 172222/GenBank KC841345. 3 km E Amaybamba: MVZ 174053/GenBank M35702.

Akodon varius (12 specimens): **BOLIVIA**: CHUQUISACA: Rio Limon: MSB 63483/MSB NK 21723/GenBank EU260478. Rio Limon, 1,300 m: AMNH 262675/MSB NK 21740/GenBank EU260479. COCHABAMBA: 25 km SW of Cochabamba, 2750 m: FMNH 21560; FMNH 50982; FMNH 50983; FMNH 50979; FMNH 51929; FMNH 50977; FMNH 50980; FMNH 50981; FMNH 50160; FMNH 50978.

Oxymycterus paramensis (1 specimen): **PERU**: CUSCO: 55.4 km by rd. N Calea, 3560 m: UMMZ 160535/GenBank UO3536.